A simple new approach predicting how microalgae culture systems will perform under sunlight and artificial light conditions

Jeremy Pruvost, R. Rasheed, Khadija Samhat, A. Kazbar, H. Al Jabri, Jérémi Dauchet, Jean-François Cornet

Algal Research 80 (2024) 103517

Contents lists available at ScienceDirect

Algal Research

journal homepage: www.elsevier.com/locate/algal

A simple new approach predicting how microalgae culture systems will perform under sunlight and artificial light conditions

J. Pruvost [a,*], R. Rasheed [b], K. Samhat [a], A. Kazbar [c], H. Al Jabri [b], J. Dauchet [d], J.F. Cornet [d]

[a] GEPEA, Université de Nantes, ONIRIS, CNRS, UMR6144, bd de l'Université, CRTT - BP 406, 44602 Saint-Nazaire Cedex, France
[b] Qatar University, Center for Sustainable Development, Qatar
[c] Wageningen University, Bioprocess engineering group, the Netherlands
[d] Université Clermont Auvergne, Clermont Auvergne INP, CNRS, Institut Pascal, F-63000 Clermont-Ferrand, France

ARTICLE INFO

Keywords:
Photobioreactors
Scaling
Microalgae
Maximal productivity
Optimization

ABSTRACT

There are many problems associated with the methods for scaling microalgae culture systems. Mathematical models - predictive models in particular - are considered key, but most of them require specialist programming and computer science skills. Even where these skills are available, new parameters (such as radiative properties for determining the effect of light attenuation on photosynthetic growth) have to be determined with each application of the model for a new strain of microalgae, and this in itself is highly complex. Consequently, the methods used in the field are still mainly (semi-)empirical. A simplified method of determining maximal performance and the corresponding optimal operating points (i.e. biomass concentration, harvesting rate) for a given culture system, strain and culture condition (including solar) is presented here. The approach involves engineering equations, which are smartly adapted in this study to eliminate parameters that are difficult to obtain, with a few conventional small-scale experiments to determine the remaining key parameters relevant to the strain. The method is applied with two strains: *Haematococcus pluvialis* (in green phase and under continuous light) and a *Picochlorum maculatum* strain isolated from the Qatar desert (in both continuous and diurnal light cycles). A deviation of <10 % was achieved between the predicted data and the experimental data. The proposed method, which eliminates several months of experiments and is relatively simple to apply, appears to be an appropriate tool for optimizing and accelerating the scaling-up of microalgae culture systems.

1. Introduction

The potential of microalgae is now recognized in many fields, including food, biofuel and the treatment of effluent [1–5], but scaling up is still a major challenge. In addition to the technical issues involved with the cultivation process and robustness of large-scale cultures, there is still a lack of simple engineering tools to scale the production facilities for a given strain. This is particularly the case for scaling up the production of less-well-documented species, as the available studies are usually conducted at lab scale (<1 L).

Mathematical models, in particular models for predicting microalgae culture systems, are considered key [6–11]. Much progress has been made in recent years and modeling can now provide solutions, for example, for determining biomass productivity and predicting the influence of operating parameters such as light supply (i.e. hemispherical incident photon flux density; hereafter PFD) and harvesting strategy (i.e. dilution rate D) [12–15]. However, theoretical tools for robust and reliable transfer from laboratory to industrial scale remain few, especially in the case of solar conditions, since a significant variation in solar radiation makes it difficult to predict the performance in a given place or for a full year of operation. Unlike conventional bioprocesses such as fermenters, therefore, where performance (productivity) in terms of volume is usually easy to predict, it is still challenging for microalgae and photosynthetic production.

Much of the problem is due to the complex relationship between incident light, light attenuation in the culture volume, and resulting photosynthetic growth. The aim of the majority of available models is to predict this relationship as accurately as possible, as an essential step towards determining the productivity of a given culture system according to species, light received, culture system geometry (i.e. culture thickness) and culture operation (dilution rate, for example).

Cornet and Dussap [16] developed engineering equations to determine the maximum productivity of culture systems analytically. These

* Corresponding author.
E-mail address: Jeremy.pruvost@Univ-Nantes.fr (J. Pruvost).

https://doi.org/10.1016/j.algal.2024.103517
Received 8 December 2023; Received in revised form 15 April 2024; Accepted 20 April 2024
Available online 25 April 2024

Nomenclature

$\mathscr{A}$	local volumetric rate of photon absorbed [μmol.s^{-1}.m^{-3}]
A	local specific rate of photon absorbed (RPA) [μmol.s^{-1}.kg^{-1}]
A_c	specific rate of photon absorbed at compensation point [μmol.s^{-1}.kg^{-1}]
a_{light}	specific illuminated area for the photobioreactor [m^{-1}]
b	back-scattered fraction for radiation [dimensionless]
C_x	biomass concentration [kg.m^{-3}]
D	dilution rate [h^{-1} or s^{-1}]
E_a	mass absorption coefficient [m^2.kg^{-1}]
E_s	mass scattering coefficient [m^2.kg^{-1}]
f	forward scattered fraction for radiation [dimensionless]
f_d	volume dark fraction of the photobioreactor [dimensionless]
G	local spherical irradiance [μmol.s^{-1}.m^{-2}]
I	intensity or luminance [μmol.s^{-1}.m^{-2}.sr^{-1}]
K	half saturation constant for photosynthesis [μmol.s^{-1}.m^{-2}]
ka	linear absorption coefficient [m^{-1}]
$kext$	linear extinction coefficient [m^{-1}]
ks	linear scattering coefficient [m^{-1}]
L	depth of the rectangular photobioreactor or the spectrophotometer cuvette [m]
M_x	C-Molar mass [kg$_X$.mol$_X^{-1}$]
n	degree of collimation for solar radiation [dimensionless]
OD	optical density or absorbance [dimensionless]
p_λ	photon distribution function for sources [μmol$_{h\nu}$.nm^{-1}]
p_A	absorptivity [dimensionless]
q	hemispherical photon flux density on a given surface (PFD) [μmol$_{h\nu}$.s^{-1}.m^{-2}]
P_V	biomass volumetric growth rate (productivity) [kg.m^{-3}.s^{-1} or kg.m^{-3}.h^{-1}]
R_λ	reflectance [dimensionless]
S_L	illuminated surface of the photobioreactor [m^2]
P_S	areal biomass productivity [kg.m^{-2}.d^{-1}]
T_λ	transmittance [dimensionless]
V_D	volume of the photobioreactor not lit by the incident PFD [m^3]
V_L	volume of the photobioreactor lit by the incident PFD [m^3]
$V_R = V_L + V_D$	total photobioreactor volume [m^3]
x_d	diffuse fraction for incident PFD at any location [−]
z	depth of culture or length [m]

Greek letters

α	linear scattering modulus [dimensionless]
β	inclination of the photobioreactor surface, [rad]
γ	fraction for working illuminated volume in the photobioreactor [dimensionless]
δ	extinction coefficient for the two-flux method [m^{-1}]
θ	incident angle (defined from the outward normal of the illuminated surface of the culture system), [rad]
ρ_M	maximum energy yield for photon conversion [dimensionless]
$\overline{\phi'_X}$	mean mole quantum yield for the *Z*-scheme of photosynthesis [mol$_X$.μmol$_{h\nu}^{-1}$]

Subscripts

NH	related to normal-hemispherical quantity
opt	related to optimal value for residence time
θ	related to angular polar quantity

Abbreviations

PAR	photosynthetically active radiation
PBR	photobioreactor
PFD	photon flux density

equations were derived from a whole corpus of theoretical knowledge developed for photobioreactor modeling [16] over the last few decades in the context of life-support systems studies by the European Space Agency (ESA). They can only calculate the maximum productivity for a given strain, N-source, culture system, and lighting condition, so any growth limitation or failure to work under optimal light attenuation conditions (at optimal biomass concentration, see below), will lead to a lower kinetic performance. Nevertheless it is essential for the engineer to know its maximum performance, as with any industrial system, as this informs the sizing of the installation and identification of any growth limitation that may occur, by comparing it with actual results [17,18].

The validity of these equations has been demonstrated in several works, using cyanobacteria, microalgae, photobioreactors of different tubular and flat geometry, and artificial light and solar conditions [12,16,17,19–21]. In each case, a maximum deviation of 15 % was achieved, compared to the results of the experiment or complete simulation model, and this is largely acceptable for an engineer.

The major drawback with the equations is the need for several parameters, the identification of which requires significant upstream study using special equipment and methods, although they are otherwise easy to measure. This is the case, for example, with identifying radiative properties, which involves significant experimental or theoretical work [22–26].

This article presents a simplification of the available equations and models in order to predict essential data such as maximal biomass productivity and corresponding optimal operating conditions quickly (i.e. optimal biomass concentration and dilution rate), without significant upstream development or expensive equipment. Engineering equations smartly adapted to eliminate parameters that are difficult to obtain are combined with a few conventional lab-scale experiments to determine the remaining key parameters relevant to the strain for a given incident field of radiation (spectral, angular and energy distribution). In order to illustrate the genericity of the method, three microalgae species cultivated in different conditions and photobioreactor (PBR) geometries will be considered. The green microalga *Chlorella vulgaris* will initially be used as a model species for the implementation of the method, all requested information to simulate various cases being available elsewhere (see Section 3.1). Then, illustrations of applications of the method will be given for two cases: *Haematococcus pluvialis* (here cultivated in green phase) as a strain with already recognized industrial interest (Section 3.2) and *Picochlorum maculatum* a recently isolated strain from the Qatar desert with high potential for developing aquaculture in harsh desert conditions (Section 3.3). Those choices will allow illustrating applicability to the method to both artificial continuous light and diurnal light cycles.

2. Theoretical considerations

2.1. Theoretical background: General equations for determining biomass productivity

The productivity of biomass is essential information with any culture system. With microalgae, areal productivity P_S (g.m^{-2}.d^{-1}) is used in addition to volumetric productivity P_V (g.m^{-3}.d^{-1}) due to the need for surface illumination. They are linked by the geometric characteristics of the culture system, in particular the specific illuminated surface a_{light} defined by the ratio of illuminated surface S_{light} on the illuminated volume of culture V_L ($a_{light} = S_{light}/V_L$):

$$P_s = \frac{P_v\, V_L}{S_{light}} = \frac{P_V}{a_{light}} \quad (1)$$

Cornet and Dussap [16] developed engineering equations to estimate the maximum volumetric biomass productivity P_V, and following that, the maximum biomass areal productivity $P_{S\ max}$ from characteristics relevant to the strain, the culture system, and the conditions of use, using Eq. 1. This is given by:

$$P_{S\ max} = (1-f_d)\rho_M M_X \overline{\phi_X^{'}} \frac{2\alpha}{1+\alpha} \frac{K}{\left(\frac{n+2}{n+1}\right)} ln\left[1 + \frac{\left(\frac{n+2}{n+1}\right) q_0}{K}\right] \quad (2)$$

The parameters for Eq. 2 can be divided into three groups:

- *Parameters related to species*: these include the biomass mole quantum yield for the *Z*-scheme of photosynthesis $\overline{\phi_X^{'}}$, the C-molar mass M_X, the half-saturation constant for photosynthesis K, and the linear scattering modulus α related to the radiative properties of the microorganism.

- *Parameters related to operating conditions*: the total incident PFD q (expressed here in $\mu mole_{h\nu}.m^{-2}.s^{-1}$ on the PAR - photosynthetic active radiation - corresponding to the 400–700 nm spectral range) and the degree of collimation of incident radiation n, varying between $n = 0$ for diffuse radiation and $n = \infty$ for collimated radiation.

- *Parameters related to culture system geometry*: the dark volume fraction in the design f_d ($f_d = V_D/(V_L + V_D)$) which represents any volume fraction of the culture system not lit by the incident PFD (V_D) owing to system design, e.g. having a recirculating tank.

As explained by the authors in their funding paper, the maximum primary quantum yield $\rho_M \cong 0.8$, and the linear scattering modulus related to the radiative properties of the microalgae $\alpha = 0.85–0.9$ have extremely robust values for any photosynthetic microorganism. It can also be observed that all these parameters for a given species (and therefore with fixed, species-related parameters) are linked to light. This concurs with the fact that maximal performance is obtained at optimal operating conditions, where light alone limits growth (hereafter "light-limited growth"), assuming all other biological needs (nutrients, dissolved carbon, etc.) and operating conditions (pH, temperature, etc.) are controlled at optimal values [10,27].

In addition, the maximal biomass productivity, as predicted using Eq. 2, was also obtained for a given biomass concentration (i.e. the optimal concentration) as with any bioprocess. With the culture of photosynthetic microorganisms, obtaining this last condition is far from simple as it is associated with optimal light absorption conditions, this being a function of incident light, biomass concentration and cell pigmentation (i.e. radiative properties). This has been widely discussed by authors in several publications [17,28,29].

Obtaining these optimal light attenuation conditions in practice for a given strain and culture system can be tricky. Even under optimal operating conditions (light-limited growth), a significant difference is obtained between the productivity observed and the maximum possible values. This is particularly true for microalgae, due to the influence of strong light attenuation (dark volume) on the amount of respiratory activity in light on the overall kinetic performance of the culture system (i.e. the growth rate). Takache et al. [14,21] provide more details on this. It will be discussed further in this work, and a method for estimating optimal biomass concentration will be presented, as a prerequisite to obtaining maximal biomass productivity in the culture system.

Eq. 2 also reveals an interesting property: the maximum areal productivity $P_{S\ max}$ for a strain and a given incident flux (PFD) does not depend on the geometry of the culture system (except for the f_d value, which is fixed by the design of the culture system). This is also true without the light attenuation condition, leading to maximum productivity [15]. Therefore, when operating a culture system in continuous mode at a given dilution rate D ($D = Q/V_R$ with Q the liquid flow rate of the feed and V_R the total volume of the culture system) and incident PFD, a constant biomass concentration will be reached (steady state), enabling determination of the experimental areal biomass productivity:

$$P_s = \frac{C_x.Q}{S_{light}} = \frac{C_x\, D\, V_R}{S_{light}} = \frac{C_x\, D}{a_{light}} \quad (3)$$

If we consider, in the first instance, the usual case of a cultivation system with no dark fraction ($f_d = 0$) in the design, the experimental areal biomass productivity thus determined will be similar for other culture systems with different specific illuminated surfaces (i.e. different culture thicknesses) but operated under the same PFD and dilution rate. This constant areal biomass productivity property can be combined with Eq. 1 on volume productivity to express the relationship between two culture systems with different specific illuminated surfaces a_{light}, as follows:

$$P_{s,1} = P_{s,2} = \frac{P_{v,1}}{a_{light,1}} = \frac{P_{v,2}}{a_{light,2}} \quad (4)$$

where $P_{V\,1}$ and $P_{V\,2}$ are the biomass volume productivities of the two culture systems with specific illuminated surfaces $a_{light\,1}$ and $a_{light\,2}$ respectively.

An initial, simple engineering equation can thus be introduced to determine the volumetric productivity P_V of any culture system ($P_{v,2}$) from a measurement obtained from a given culture system ($P_{v,1}$):

$$P_{v,2} = P_{v,1} \frac{a_{light,2}}{a_{light,1}} \quad (5)$$

With a flat-panel PBR, for example, the specific illuminated surface is given by $a_{light} = \frac{S_{light}}{V_R} = \frac{1}{L}$, where L is the depth of the culture system. The biomass volume productivity $P_{v,2}$ of a PBR (PBR#2) can then be determined from the experimental value $P_{v,1}$ obtained for a given PBR (PBR#1), and the ratio of the depths of the PBRs $\frac{L_1}{L_2}$:

$$P_{v,2} = P_{v,1} \frac{L_1}{L_2} \quad (6)$$

It is possible, therefore, to extrapolate productivity to a larger-scale culture system (PBR#2) using measurements obtained from a PBR at laboratory scale (PBR#1). This approach was used by Pruvost et al. [18] to extrapolate the culture of *Neochloris oleabundans* from a 1-l flat-panel airlift PBR to a 130-l PBR, and was also demonstrated by Busnel et al. [15]. It has also been combined more recently with the use of LED panels to simulate solar cycles, in order to estimate the productivity of solar raceway systems from data obtained in the laboratory [30].

Note that the approach can easily be extended to cultivation systems presenting a design dark fraction ($f_d \neq 0$, leading therefore to $P_{v,2} = P_{v,1} \frac{L_1}{L_2} \frac{f_{d,2}}{f_{d,1}}$).

2.2. Proposal for development

2.2.1. Simple estimation of maximal biomass productivity

Although fully predictive, Eq. 2 involves filling in several parameters, some being rather difficult to obtain, especially those related to species. The method for determining these parameters is fully detailed in the literature, but obtaining them requires a set of experiments involving specific equipment and time-consuming measurements [13,14].

The objective here is to propose a simplified approach combining simple experiments with the theoretical basis provided by Eq. 2. The general principle is to carry out an experimental determination of some maximum areal biomass productivities obtained for different PFD values. One key element that differs between microalgae strains, in addition to the different growth rates under given light conditions, is the evolution of this growth rate with light. Reformulating Eq. 2 for with different PFD values q_1 and q_2 leads to:

$$\frac{P_{s\ max1}}{P_{smax2}} \approx \frac{ln\left[1+\frac{q_1}{K'}\right]}{ln\left[1+\frac{q_2}{K'}\right]} \tag{7}$$

Note that with Eq. 7, the determination of parameters that can prove difficult is simplified; this concerns both radiative properties and biological parameters related to species. One constant only, denoted K', is required, which can be estimated through experiments (as explained below, this constant is slightly different from the exact value of the half-saturation constant for photosynthesis K obtained by independent experiments but may be considered as a first good approximation).

Eq. 7 assumes that the dark fraction f_d and degree of collimation for incident radiation are constant. This is true when extrapolating values from different PFDs for the same culture system, but if the aim is to apply the approach to different culture systems with different dark fractions f_d or different incident light conditions, the method can simply be extended using the same approach:

$$\frac{P_{s\ max1}}{P_{Smax2}} \approx \frac{(1-f_{d\,1})}{(1-f_{d\,2})} \frac{\left(\frac{n+2}{n+1}\right)_2 ln\left[1+\frac{\left(\frac{n+2}{n+1}\right)_1 q_1}{K'}\right]}{\left(\frac{n+2}{n+1}\right)_1 ln\left[1+\frac{\left(\frac{n+2}{n+1}\right)_2 q_2}{K'}\right]} \tag{8}$$

2.2.2. Limitations of the approach

Although the equations are derived from a reliable, detailed modeling corpus, the general aim here is to propose simplified engineering equations, and there are limitations and assumptions with the ones above.

The first assumption is that the strain-related parameters are constant with the incident flux, in terms of the linear scattering modulus α in Eq. 2 in particular. As mentioned above, Cornet and Dussap [16] suggest that the expression of absorption and scattering coefficients in the form of the linear scattering modulus α leads to an almost constant and robust value between strains, and a fortiori between culture conditions for a given strain. The term $\frac{2\alpha}{1+\alpha}$, representing the part (1 – Reflectivity) of incident photons actually entering the liquid medium of the culture system can therefore generally be taken as 0.85–0.95.

Another limitation of the approach is that it applies only to maximum biomass productivity (Eq. 7 and Eq. 8, as well as Eq. 2 for which they are derived). Calculation of the constant K' in Eq. 7 and Eq. 8 therefore requires determination of the experimental values for maximum biomass productivity of the strain with a given PFD value. As discussed above, this involves (i) obtaining the light-limited growth where only the light supply limits growth (i.e. no limitation of growth by nutrients, dissolved carbon, optimized pH or temperature) and (ii) determining the optimal biomass concentration, for example by varying the dilution rate in a continuous culture.

Since it is not easy to achieve the condition of optimal biomass concentration, a simplified approach to estimating the values for various PFDs and culture systems has also been developed (see below), bearing in mind that Eq. 7 and Eq. 8 are only valid for determining maximal biomass productivity.

2.3. Extension to the case of biomass productivity under solar conditions

An evolution of Eq. 2 for solar conditions was proposed by Pruvost et al. [17]. This equation introduces the specificities of sunlight use, leading to:

$$P_{s,max} = (1-f_d)\rho_M M_X \overline{\phi_X^{\cdot}} \frac{2\alpha}{1+\alpha} \frac{\overline{x_d}K}{2}\left[ln\left[1+\frac{2\overline{q}}{K}\right]+(1-\overline{x_d})\overline{cos\theta}Kln\left[1+\frac{\overline{q}}{K\overline{cos\theta}}\right]\right] \tag{9}$$

The location, time of year, and ability of the cultivation system to collect light are accounted for by (a) $\overline{x_d}$, the mean fraction of diffuse radiation in the total incident solar flux density (PAR), typically around 0.1–0.5, (b) the mean cosine of the incident angle θ onto the culture system surface $\overline{cos\theta}$ - usually within the range 0.4 to 0.7, and (c) the incident PFD $\overline{q}$ (here indicates that all values are time-averaged in a given operating period. Note that because all values rely on only light-related parameters, the averaging should be done only in the daytime, to the exclusion of all nighttime periods - see below for example). From Eq. (2), the degree of collimation has been taken respectively as $n = 0$ for diffuse Lambertian radiation (leading to the term $2\overline{q}$) and to $n \to \infty$ for direct collimated incident radiation. These two assumptions represent the two extremes for the angular distribution of any incident PFD and are therefore appropriate for depicting incident solar light (see Appendix A for details).

Eq. 9 ultimately enables predictive determination of the biomass productivity (surface and volume, using Eq. 1) for a given period of the year (including the whole year) for any location, using solar information obtained from a meteorological database [12,17].

Using the same method as for Eq. 7 and Eq. 8, the following simplified equations are obtained for solar culture systems with engineering dark fraction f_d (Eq. 10a) or without it (Eq. 10b):

$$\frac{\overline{P_{Smax1}}}{\overline{P_{Smax2}}} \approx \frac{(1-f_{d1})\left[ln\left[1+2\frac{\overline{q_1}}{K'}\right]+(1-\overline{x_{d1}})\overline{cos\theta_1}K'ln\left[1+\frac{\overline{q_1}}{K'\overline{cos\theta_1}}\right]\right]}{(1-f_{d2})\left[ln\left[1+2\frac{\overline{q_2}}{K'}\right]+(1-\overline{x_{d2}})\overline{cos\theta_2}K'ln\left[1+\frac{\overline{q_2}}{K'\overline{cos\theta_2}}\right]\right]} \tag{10a}$$

$$\frac{\overline{P_{Smax1}}}{\overline{P_{Smax2}}} \approx \frac{\left[ln\left[1+2\frac{\overline{q_1}}{K'}\right]+(1-\overline{x_{d1}})\overline{cos\theta_1}K'ln\left[1+\frac{\overline{q_1}}{K'\overline{cos\theta_1}}\right]\right]}{\left[ln\left[1+2\frac{\overline{q_2}}{K'}\right]+(1-\overline{x_{d2}})\overline{cos\theta_2}K'ln\left[1+\frac{\overline{q_2}}{K'\overline{cos\theta_2}}\right]\right]} \tag{10b}$$

As for Eq. 7, only one parameter (K'), related to the species, remains. This is particularly noteworthy in the context of solar production, as it means these equations allow the maximum productivity to be determined for a given solar cycle (i.e. fraction of diffuse radiation $\overline{x_d}$, cosines of incident angle θ and incident PFD $\overline{q}$; all values averaged for a given daily period of operation). As illustrated below, the determination of K' from lab-scale experiments (even in continuous light using Eq. 2) will enable extrapolation of the maximal biomass productivity for a whole year, but it could also be used to predict performance in other places of production, or with different technologies (including different sunlight orientation and inclination of the solar culture system).

2.4. Determination of optimal biomass concentration

Light-limited growth is a necessary but inadequate condition for achieving maximal biomass productivity in a given culture system. Appropriate light transfer (or light attenuation) conditions must also be established within the culture volume. Other publications go into more detail on this [16,21,31]. To summarize, the biomass concentration must be high enough to absorb incoming photons, while for microorganisms with non-negligible respiration activity under illumination, such as eukaryotic microalgae, a dark volume in the culture volume, such as results from an over-large biomass concentration, should be avoided. Achieving the maximum kinetic performance (i.e. biomass productivity) for a given PFD value therefore requires the precise condition of complete absorption of the incident light, but with no dark volume in the culture volume. This condition is often referred to as the *luminostat* mode. It has also been introduced as the "$\gamma = 1$" condition,

where γ is the ratio of the illuminated volume to the total volume of the culture [21,32]. Note that for microorganisms with negligible respiration activity under illumination, such as prokaryotic cyanobacteria cells, fulfilling the condition of complete light absorption ($\gamma \leq 1$) is sufficient to achieve maximum biomass productivity.

To obtain optimal light attenuation conditions to be achieved with the culture system, the culture system must be operated at the optimal biomass concentration, here noted $C_{x,opt}$ (and other optimal culture conditions such as pH, temperature, medium, etc.). The relationship between light attenuation conditions and productivity of a culture system has been widely discussed by the authors Pottier et al. [26] and Dauchet et al. [23]. With a continuous culture system, this is obtained by adjusting the dilution rate to obtain the value for optimal biomass concentration in the culture system. This is illustrated in Fig. 1, where biomass productivity is given as a function of dilution rate (Fig. 1-a) and biomass concentration (Fig. 1-b). Maximum productivity thus corresponds to an optimum dilution rate and an optimum biomass concentration (the two being related). These values are also dependent on the PFD q applied onto the culture system.

As mentioned above and illustrated in Fig. 2, the optimal light attenuation condition corresponds to full light attenuation with no dark volume. For microalgae, a dark volume corresponds to a part the culture volume where the light received is insufficient for positive growth. This is known as the compensation point of photosynthesis (noted A_c), which defines the minimum rate of photon absorption (RPA) necessary for net positive photosynthetic growth (the calculation of RPA will be detailed below, see Eq. 11). A specific, easy-to-use parameter called the "illuminated volume fraction", denoted γ, can be introduced here

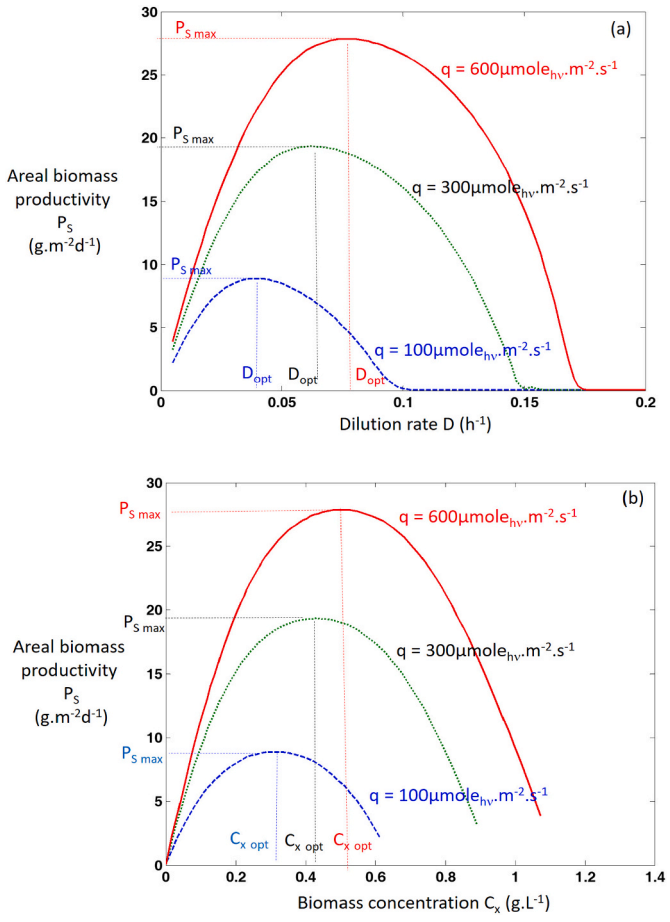

Fig. 1. Areal biomass productivity evolution as a function of the dilution rate (1-a) and biomass concentration (1-b) in continuous culture of *Chlorella vulgaris* for various PFD values.

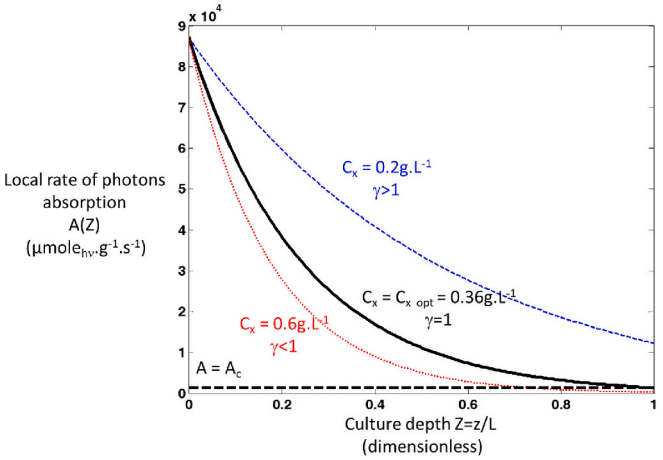

Fig. 2. Light attenuation profiles in a flat panel photobioreactor obtained for different biomass concentration (q = 300µmole$_{hv}$.m^{-2}.s^{-1}).

[16,28,33,34]. Schematically, the culture mass can be divided into two zones - an illuminated zone and a dark zone. The illuminated volume fraction γ is given by the depth of the culture z_c, where the local value of RPA (denoted $A(z)$) corresponds to the compensation point of photosynthesis (i.e. $A(z_c) = A_C$). Consequently, the optimal light attenuation condition corresponds to "$\gamma = 1$", indicating full light absorption with no dark volume (no RPA value in the culture volume below compensation point A_C). Other light attenuation regimes are also given, for information, in Fig. 2, as obtained with (i) a biomass concentration which is too large, leading to a dark volume ($\gamma < 1$) and (ii) a biomass concentration which is too low, preventing full light attenuation ($\gamma > 1$, the length z_c appearing here rather as an extinction length, which would require a greater thickness L of the culture system depth to absorb all the incident radiation).

As a new development, we propose here to make the condition $\gamma = 1$ (i.e. optimal light attenuation condition) reliant on determination of the compensation point A_C - which is characteristic of a given strain - as a key value for estimating the optimal biomass concentration and therefore the corresponding dilution rate for any light condition or culture thickness.

Previous works have demonstrated the importance of the two-flux approximation when proposing light transfer models for microalgae culture, taking into account both absorption and scattering phenomena as induced by microalgae cells. The main drawback with this approach is the need to determine the related radiative properties, i.e. absorption and scattering coefficients, as well as the backscattered fraction which issues from the cell phase function. These values can be obtained either experimentally or theoretically (for a review of these two approaches, see Dauchet et al. 2015), but they are not easy to determine.

Keeping to the idea of defining a simple engineering method, we used the approach introduced by Cornet and Dussap [16], also used by Kandilian et al. [35], where the contribution of scattering was disregarded in the light transfer equation, leading to a formulation for the radiative transfer in a purely absorbing medium. Additionally, this absorbing medium is considered as a grey medium with a mean mass absorption coefficient Ea, obtained by averaging the spectral value of Ea_λ in the PAR from the source energy and its light spectrum ([26]; see also appendix B).

For culture systems of Cartesian geometry, with light attenuation occurring along one direction (i.e. rectangular geometries such as flat panels or raceway culture systems), this simplification was able to successfully estimate the rate of photon absorption $A(z)$, as given by:

$$A(z) = Ea.G(z) \cong Ea.q.e^{-Ea.Cx.z} \quad (11)$$

Note that this expression is only valid for quasi-collimated incident

PFDs, which is a good assumption for many practical cases. As detailed in Appendix A, it can be generalized (for solar diffuse radiation or artificial one with incident beam angles higher than 20°) with any degree of collimation of the incident radiation leading to (see appendix A for details):

$A(z) = Ea\,(n+2)q\,\mathrm{E}_{n+2}(Ea \bullet C_X \bullet z)$ (Eq. A 12 in appendix) in which the $\mathrm{E_n}$ function is the $\mathrm{n^{th}}$ order integral exponential function available in many languages. As explained in Appendix A, the well-known expression of the local RPA in a quasi-collimated incident PFD (Eq. 11) can be determined by taking the limit $n \to \infty$. Using the property of the $\mathrm{E_n}$ function $\lim_{n\to\infty} N\,\mathrm{E}_n(x) = \mathrm{e}^{-x}$ leads directly to the well-known Bouguer law in this case (often called the Lambert-Beer law), and therefore to Eq. 11.

Note also that, as discussed in Kandilian et al. [35], the method can be conveniently combined with an experimental determination of the absorption cross-section *Ea* using a spectrophotometer equipped with an integrative sphere. This approach, based on normal hemispherical transmittance, enables simple, accurate determination of the absorption cross-section *Ea* (see Appendix B for details of the experimental method).

By expressing Eq. 11 for the specific condition $\gamma = 1$ (minimum value of RPA equal to A_c as achieved at the back of the culture volume $z = L$), the optimal biomass concentration $C_{x,opt}$ can be related to the quantity A_C by:

$$A_c \approx A(L) = Ea.q.e^{-Ea.C_{x,opt}.L} \tag{12}$$

Eq. 12 therefore enables estimation of the compensation point of photosynthesis A_c from measurements of $C_{x,opt}$ at a given PFD value q (as obtained at maximal productivity, see below for an example of application), and mass absorption coefficient *Ea*. Once the value of the compensation point of the cultivated stain is known, Eq. 12 can then be used to estimate the optimal biomass concentration for different PFDs or different culture system depths:

$$C_{x,opt} \approx \frac{1}{Ea.L} ln\left(\frac{Ea.q}{A_c}\right) \tag{13}$$

Although Eq. 13 can be used directly, the concept of "areal biomass concentration (in $\mathrm{g.m^{-2}}$)" can be introduced here. Its significance was proved by Lee et al. [36] and Hoeniges et al. [37], where it was shown that, when expressed per unit of illuminated surface, an optimal areal biomass concentration value (noted $C^s_{x,opt}$) could be defined whatever the culture system depth when operated at a given PFD value:

$$C^s_{x,opt} = C_{x,opt}\frac{V_R}{S_{light}} = C_{x,opt}\,L \approx \frac{1}{Ea} ln\left(\frac{Ea.q}{A_c}\right) \tag{14}$$

Note that Eq. 14 gives the relevance of light absorption in a microalgae culture system. Maximal kinetic performance (i.e. maximal biomass productivity and therefore average growth rate on the culture volume) at a given PFD is obtained at an optimal areal biomass concentration $C^s_{x,opt}$, which depends on its absorption coefficient. In other words, a sufficient absorption per unit of cultivated area is necessary to obtain maximal performance of the culture system. This way of reasoning in the field of microalgae cultivation is very similar to the reasoning in absorption optical thickness in the field of radiative transfer [23]. For a given absorption coefficient *Ea*, it is well known that the absorption in any photo(*bio*)chemical process is controlled by the absorption optical thickness $\tau_{opt} = EaC_xL$. This optical thickness τ can then be optimized by adjusting either the biomass concentration $C_{x,opt}$ for a given geometry, or the culture system design (thickness L_{opt}) at a given concentration.

3. Results and discussion

3.1. Theoretical study

3.1.1. Estimation of maximum biomass productivity

To illustrate the significance of the approach, the kinetic growth model for *Chlorella vulgaris* (CCAP 211–19) developed and validated elsewhere was used to simulate various cases [13]. This detailed knowledge model is based on the same theoretical corpus used to establish our approach, enabling a reliable comparison between complete modeling and our proposed simplified engineering equations.

Fig. 1 gives the prediction of surface productivity evolution as a function of the dilution rate applied, for PFD values of between 150 and $600\mu\mathrm{mol_{h\nu}.m^{-2}.s^{-1}}$. The result of the double dependence maximum productivity on the dilution rate and PFD is clearly illustrated (Fig. 1-a). The maximum productivity $P_{S\ max}$ for each PFD was obtained for an optimal biomass concentration $C_{x,opt}$ condition (Fig. 1-b), corresponding to optimal light attenuation in the culture volume ($\gamma = 1$, Fig. 2, given for $q = 300\mu\mathrm{mol_{h\nu}.m^{-2}.s^{-1}}$), as obtained for an optimal value of dilution rate D_{opt} (Fig. 1-a). This optimal attenuation condition (and therefore D_{opt} and $C_{x,opt}$) ultimately depends on the PFD applied. Increasing the PFD will increase both the maximal biomass productivity and the optimal biomass concentration to achieve it.

Fig. 3 gives the maximum areal biomass productivity obtained for different PFD values. There is a nonlinear evolution of the maximum productivity with the PFD increase. This illustrates the expected loss of photosynthetic conversion efficiency with increasing light received. Therefore, even if the productivity continues to increase with the increase of PFD, the energy dissipation is greater [10,20,29,38]. In Eq. 7, this evolution is represented by the logarithmic formulation and the K' value (the higher the K' value, the lower the decrease in efficiency, indicating greater resistance of the strain to light).

Following Eq. 7, two values of maximal biomass productivity were used to determine the value of K': $P_{s\ max1} = 8.9\ \mathrm{g.m^{-2}.day^{-1}}$ and $P_{s\ max2} = 27.8\ \mathrm{g.m^{-2}.day^{-1}}$, as obtained for $q_1 = 100\mu\mathrm{mol_{h\nu}.m^{-2}.s^{-1}}$ and $q_2 = 600\mu\mathrm{mol_{h\nu}.m^{-2}.s^{-1}}$ respectively (Fig. 1). A value $K' = 150\mu\mathrm{mol_{h\nu}.m^{-2}.s^{-1}}$ was obtained by simple regression. Once K' was determined, it was possible to determine the $P_{S\ max}$ value for any PFD value using Eq. 7. These values were then compared to the predictions obtained by complete modeling, as in Fig. 1. The values were found to be very close (error < 2 %), as shown in Fig. 3.

Since the kinetic growth model of *Chlorella vulgaris* comes from the same theoretical corpus used to establish engineering equations, the value of K' obtained from regression can be compared to the value of the half-saturation constant for photosynthesis K used in the kinetic growth model ($K = 110\mu\mathrm{mol_{h\nu}.m^{-2}.s^{-1}}$, see Table 1). Different values were obtained. This is due to the hypothesis introduced in the engineering equation used to estimate maximal biomass productivity (Eq. 2, as for Eq. 10 for solar condition). As detailed in Cornet [16], several assumptions were introduced to obtain this analytical solution, producing an accuracy of 15 % compared to the complete resolution of the kinetic growth model of *Chlorella vulgaris*. This precision is quite acceptable for engineering purposes. Nevertheless, in the end, the value obtained from regression K' will necessarily be different from the half-saturation constant of photosynthesis K used in the kinetic growth model for the complete resolution of biomass concentration evolution (but generally remains within the range of 20 % uncertainty). In other words, using Eq. 7 alone (or Eq. 10 for solar conditions) does not produce the exact value of the half-saturation constant for photosynthesis K as used in the kinetic growth model, but can be used to determine the evolution of $P_{S,\ max}$ (Eq. 7 or Eq. 11 for solar condition) whatever the PFD value, which is the purpose of our approach here.

Because our method is based on the regression of only two biomass productivity values obtained with two different of PFD values, a sensitivity analysis was conducted on the prediction accuracy of K' from the maximum productivity values obtained in the regression. Since the aim

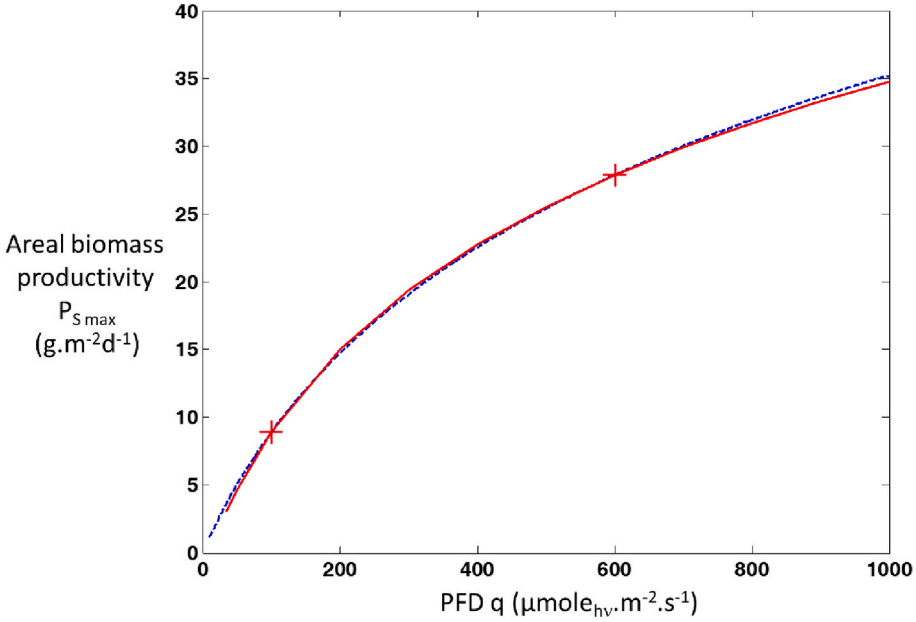

Fig. 3. Prediction of areal biomass productivity evolution as a function of PFD values for *Chlorella vulgaris* (blue dashed line: full model prediction, red solid line: prediction using Eq. 7 using values obtained at q = 100 and 600 $\mu mole_{h\nu}.m^{-2}.s^{-1}$ and for $K' = 150$ $\mu mole_{h\nu}.m^{-2}.s^{-1}$ – see text for details). (For interpretation of the references to colour in this figure legend, the reader is referred to the web version of this article.)

Table 1
Growth model parameters for *Chlorella vulgaris* used for complete simulations (values given for growth on ammonia as N-Source, see text for details).

Parameter	Value	Unit
	0.8	–
J_{NADH_2}	1.8×10^{-3}	$mol_{NADH_2}.kg_X^{-1}.s^{-1}$
υ_{O_2-X}	1.13	–
ϕ'_X	9.73×10^{-8}	$mol_X.\mu mol_{h\nu}^{-1}$
M_X	0.024	kg_X C-mol^{-1}
$\upsilon_{NADH_2-O_2}$	2	–
K	110	$\mu mol_{h\nu}.m^{-2}.s^{-1}$
K_r	0.6	$\mu mol_{h\nu}.kg^{-1}.s^{-1}$
A_c	1500	$\mu mol_{h\nu}.kg^{-1}.s^{-1}$
Ea	270	$m^2.kg^{-1}$
α	0.85	–

of the K' value is to relate the nonlinear maximum productivity evolution with the increase of the PFD, the ratio between the two PFD values used in the calculation (denoted q_1 and q_2) are of primary relevance.

Fig. 4-a gives a sensitivity analysis of the constant K' determined, with values predicted as a function of the ratio in PFD (the lower PFD q_1 was fixed arbitrarily at 100 $\mu mol_{h\nu}.m^{-2}.s^{-1}$; i.e. the same conclusion as when a different PFD is used for reference). The K' determined was highly sensitive for q_2/q_1 ratios lower than 4. For greater values, the deviation from the predicted K' value was <5 % of the value predicted for the greater simulated value ($q_2/q_1 = 10$, leading to $K' = 145$ $\mu mol_{h\nu}.m^{-2}.s^{-1}$). Fig. 4-b gives the influence on the prediction of maximal biomass productivities $P_{S\ max}$. Logically, the greater the difference between the two PFD values, the greater the precision in calculating the $P_{S\ max}$ value, due to the greater difference between the $P_{S\ max}$ values used to determine the value of K'. For high accuracy in predicting $P_{S\ max}$ values, a minimum factor of 4 is therefore recommended between the two PFD values used in Eq. 7, leading to an error of <2 %. Note also that a negligible increase in accuracy is obtained for q_2/q_1 ratios larger than 7 (error <1 %).

3.1.2. Estimation of optimal biomass concentration

As represented in Fig. 1-a, maximum productivity corresponds to optimal biomass concentration, which varies depending on the incident PFD. Estimating this optimal concentration for any condition from Eq. 13 requires knowledge of both the mass absorption coefficient Ea and the compensation point A_c. As explained in Appendix B, a simple method can be used to assess the spectral mass absorption coefficient and then its mean average grey value Ea in the PAR. The A_c value is harder to obtain. Our proposal is to estimate it from the experimental measurement of the maximum biomass productivity obtained at a given incident flux, using Eq. 13.

The sensitivity of determining it this way was first investigated. All the quantities (i.e. $P_{S\ max}$, D_{opt}, $C_{x,opt}$, A_c) were linked, but in a non-linear way, and determination of the maximum productivity can be tricky in practice [21]: if the dilution rate is too high and greater than D_{opt}, the light attenuation in the culture volume decreases, thus increasing the rate of photon absorption per cell, which can then become significant and lead to light stress [39]. This stress causes a decrease in cell pigmentation, which further decreases light attenuation, thus increasing the light absorbed per cell and therefore light stress. This results in an unstable culture regime, making it difficult to obtain the exact operating point corresponding to maximum productivity. The sensitivity of the determining A_c from Eq. 12 to identify the optimum operating point of the PBR was therefore studied.

Since the precise value of compensation point A_c is known from the *Chlorella vulgaris* kinetic growth model ($A_c = 1500$ $\mu mole.kg^{-1}.s^{-1}$, Table 1), the calculation error of compensation point A_c was determined as a function of the accuracy in determining the optimal biomass concentration $C_{x,opt}$ using Eq. 12. The results are given in Fig. 4-c. It was revealed that for accurate determination of A_c (deviation of ±20 % of the exact value) the optimal operating point must be determined at approximately 8 %, which is not straightforward experimentally, but feasible. As shown in Fig. 1-b, biomass productivities close to the maximum value can be obtained in a fairly wide range of biomass concentrations due to the bell shape of $P_{s\ max}$ evolution with biomass concentration C_x.

Once the value of A_c is known, it is then simple to determine the optimal concentration for different culture conditions from Eq. 13. Fig. 5-a gives the evolution obtained, depending on the PFD value, for

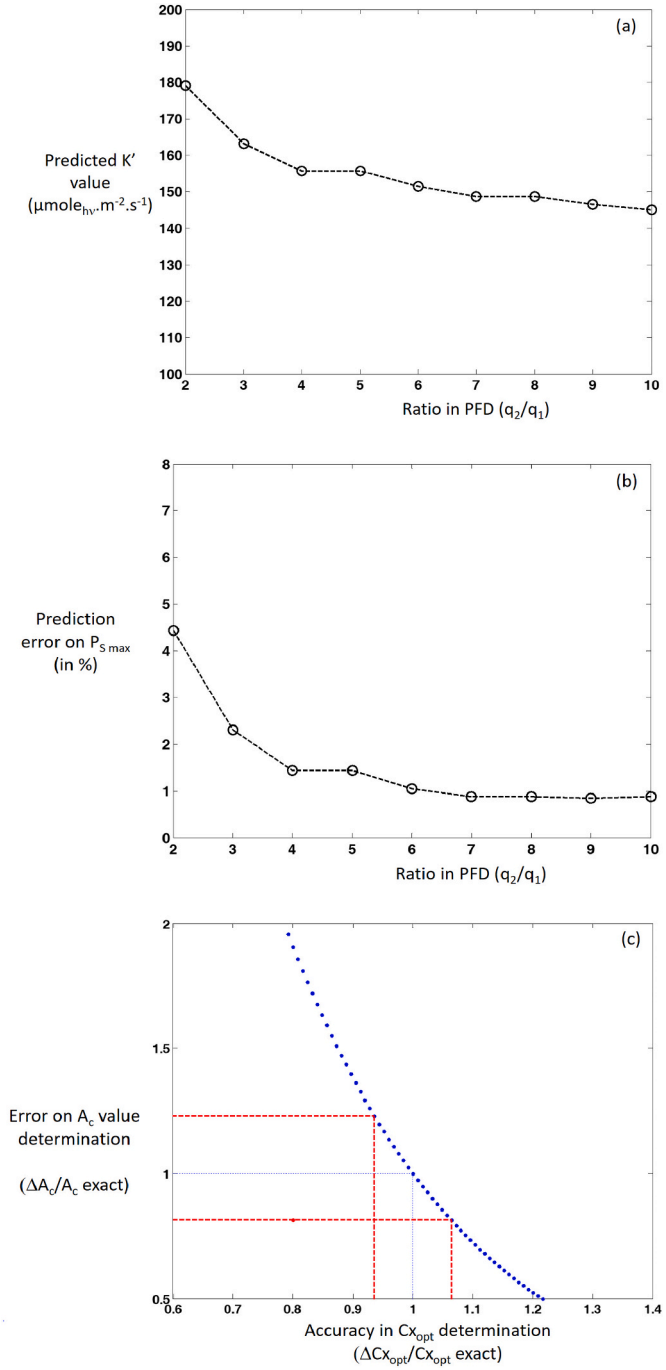

Fig. 4. Sensitivity analysis in the constant K' determination. Influence of PFD ratio in predicted K' value (4-a) and corresponding prediction error in K' estimation (4-b). Error on calculation of compensation point A_c as a function of the accuracy in determination of optimal biomass concentration $C_{X\ opt}$ (4-c).

two PBR depths: L = 0.03 m and L = 0.06 m (using the sensitivity analysis for the A_c value, an envelope corresponding to the predictions obtained with ±20 % of the A_c determination is added). Logically, the higher the PFD (or the lower the culture depth), the higher the optimal biomass concentration to obtain maximal biomass productivity. Note also that the areal biomass concentration values $C^s_{x,opt}$ for a given PFD are independent of the PBR depth when expressed per unit of illuminated surface (Fig. 5-b), confirming the significance of this quantity, as also discussed elsewhere [36,37].

Finally, it was discovered to be quite simple to determine the range of optimal biomass concentration to target in order to obtain the maximum

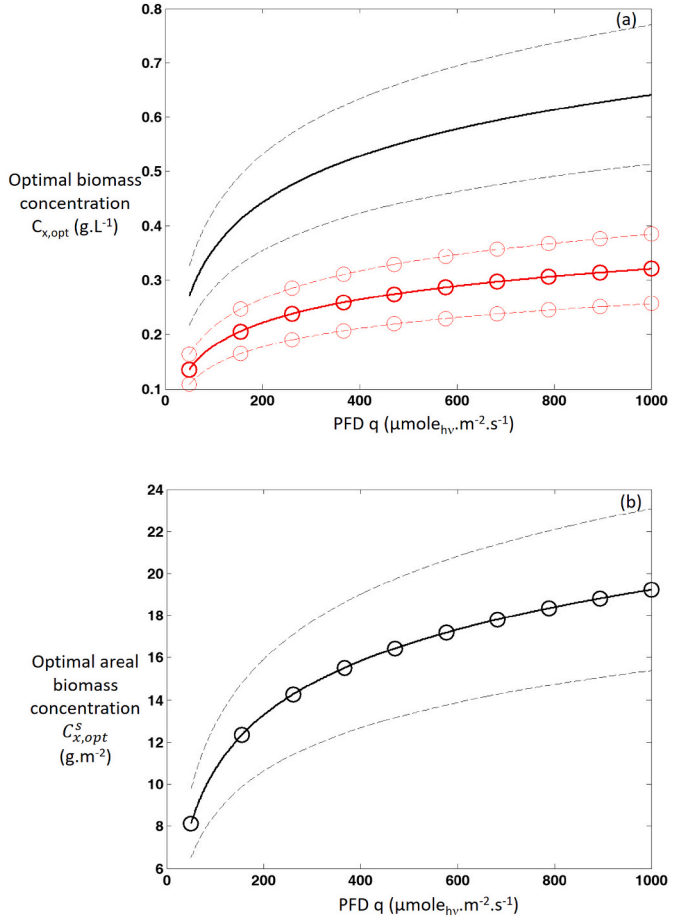

Fig. 5. Prediction of evolution of optimal concentration as a function of PFD value, as obtained from Eq. 13. Fig. 5-a gives values for two culture systems depths (red circles for L = 0.06 m; black solid line for L = 0.03 m) and Fig. 5-b gives the areal biomass concentration. Dashed lines give prediction with a ± 20 % deviation in A_c determination. (For interpretation of the references to colour in this figure legend, the reader is referred to the web version of this article.)

productivity for given operating conditions, and even if an uncertainty remains, the exact set point can be further refined through experiments.

3.2. Illustration of the significance with artificial light - Haematococcus pluvialis

3.2.1. Methodology

The method was applied on the green microalga *Haematococcus pluvialis* (SAG 34–7) grown in optimal conditions (i.e. green phase). The maximum productivity was determined for different PFD values (75–100–130–200 and 300 µmol$_{hv}$.m^{-2}.s^{-1}) by varying the dilution rate until maximum productivity was achieved for each value. Experiments were conducted in a 1 L flat-panel airlift PBR (Al-PBR, Fig. 6-a) operated continuously in chemostat mode (i.e. constant dilution rate) under different constant PFD and strict light-limited growth regimes (excess nutrients, optimum temperature and pH). Once a steady state was obtained, the dry-weight biomass concentration C_x and mass absorption coefficient Ea (Eq. 13) were determined, and biomass productivity deduced (Eq. 3). More information on the culture system, continuous operation and analysis can be obtained in Busnel et al. [15].

3.2.2. Validation of the method for maximal areal biomass productivity prediction

The maximum productivity $P_{s,max}$ values obtained were used to determine the value of the half-saturation constant for photosynthesis K'

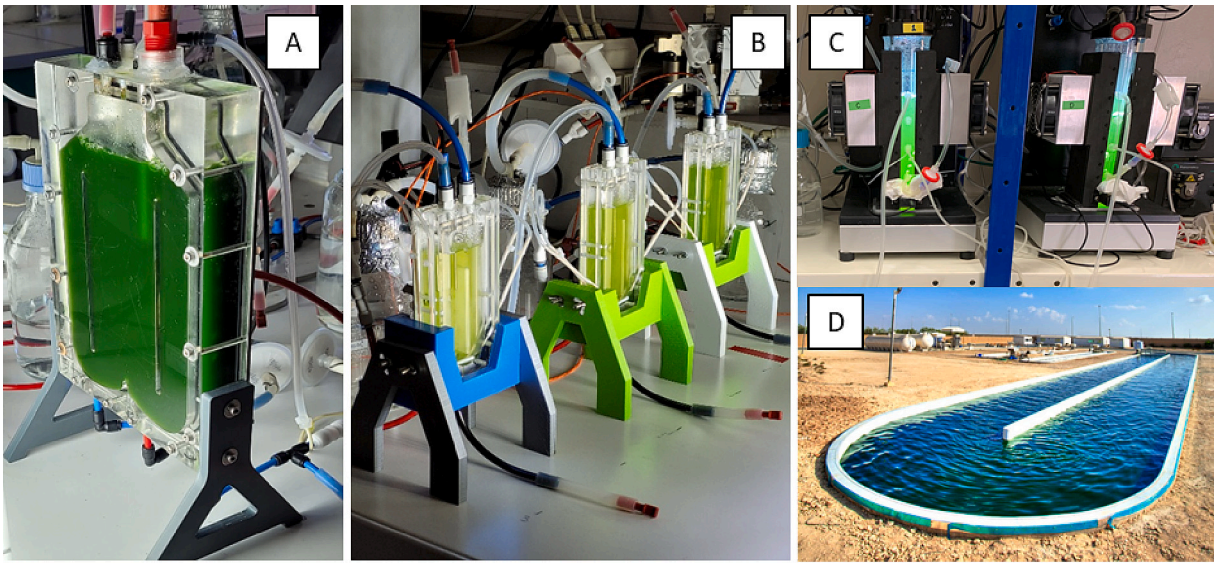

Fig. 6. Microalgae culture systems considered in the study: AL PBR (A), EOSS-2 PBR (B) ePBR (C) and outdoor raceway considered in solar simulations (D).

(Eq. 7) by simple regression. In accordance with the above recommendation on PFD ratio, the PFD values of 75 and 300 $\mu mol_{h\nu}.m^{-2}.s^{-1}$ were used here (factor 4) and a K' value of 240 ± 10 $\mu mol_{h\nu}.m^{-2}.s^{-1}$ was obtained.

By determining the value of K', the evolution of the maximal biomass productivity $P_{s,max}$ can be calculated with different PFD values. As shown in Fig. 7, there is close consistency between all the experimental and predicted values of $P_{s,max}$, with an acceptable error (< 10 %). The maximum productivity for *H. pluvialis* (green phase) can therefore be determined for any PFD value, with only two $P_{s,max}$ values at a given PFD (Eq. 7). Note that this method could save a significant amount of time; 1 to 2 months of experimentation are usually required to obtain each $P_{s,max}$ value.

3.2.3. Extension to volume biomass productivity

Once the maximal areal biomass productivities $P_{s,max}$ are known, Eq. 1 can be used to determine the maximal volume productivity $P_{v,max}$,

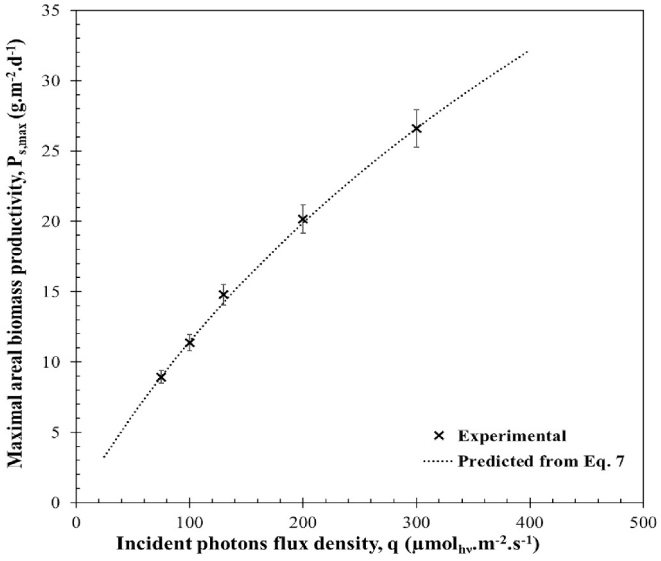

Fig. 7. Experimental and predicted values of maximal areal biomass productivity $P_{s,max}$ for *H. pluvialis* culture grown in optimal conditions in AL-PBR operated in chemostat mode, as a function of incident PFD. Experimental data shown as mean ± SD, $n = 3$.

where the specific illuminated surface of the culture system used is known. To illustrate this, *H. pluvialis* was cultivated in two different PBRs of similar geometry (flat-panel, no design dark fraction i.e. $f_d = 0$) but different depths, and therefore different specific illuminated surfaces (Al-PBR: $L = 0.03$ m, $a_{light} = 33\ m^{-1}$ and EOSS2-PBR: $L = 0.02$ m, $a_{light} = 50\ m^{-1}$, Fig. 6-a & b). The experimental results are given in Fig. 8, as well as the predictions obtained from Eq. 6.

Close agreement was observed between the experimental and predicted $P_{v,max}$ values, demonstrating that once the K' value has been determined, the simple equations proposed can be used to determine all the maximum areal and volume productivities for any incident PFD, and the specific illuminated surface a_{light}. The K' value determined here from lab-scale experiments in constant light is also valid for sunlight extrapolation, as will be shown below.

Note that if the objective is to determine volume biomass productivity for a single incident PFD, Eq. 5 is sufficient. By simply measuring the areal biomass productivity for a given PBR, therefore, any volume productivity value can be determined from the specific illuminated surface of the PBR. Note that, unlike for Eq. 7 which is only valid for maximum productivity, Eq. 5 is valid regardless of dilution rate and biomass concentration.

3.2.4. Determination of optimal biomass concentration

The prediction of optimal biomass concentration using Eq. 13 requires prior determination of the compensation point of photosynthesis A_c of the cultivated strain. This is obtained using Eq. 12, which requires experimental identification of the optimal operating conditions for maximal biomass productivity. An example of the evolution of biomass productivity with the dilution rate obtained in the Al-PBR for *H. pluvialis* at an incident PFD of 200 $\mu mol_{h\nu}.m^{-2}.s^{-1}$ is reported in Fig. 9. A maximum biomass productivity $P_{v,max}$ of 681 ± 35 $g.m^{-3}.d^{-1}$ was achieved for an optimal biomass concentration $C_{x,opt}$ of 1.29 ± 0.07 $kg.m^{-3}$ ($\gamma = 1$) and an optimal dilution rate D_{opt} of 0.022 h^{-1}. For higher dilution rates (i.e. lower biomass concentrations) there is insufficient light absorption, leading to lower biomass productivity ($\gamma > 1$) and lower dilution rates (i.e. higher biomass concentrations); a dark volume appears ($\gamma < 1$), promoting the contribution of respiration activity which also results in lower biomass productivity.

A single optimal operating point is sufficient to determine the value of A_c. However, to illustrate the reliability of our approach, the analysis was extended to both of the PBRs used in the study and other PFD values. The results are summarized in Table 2 (values of $C_{x,opt}$, D_{opt}, $P_{s,max}$ and E_a). Based on the experimental $C_{x,opt}$ and E_a values obtained for each

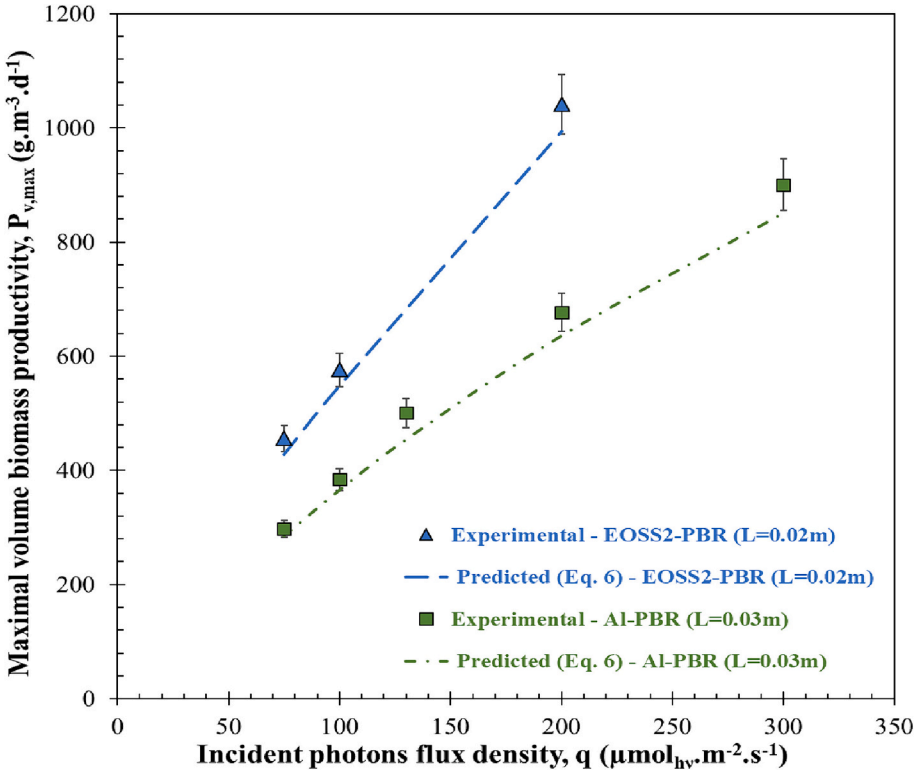

Fig. 8. Experimental and predicted values of maximal volume biomass productivity $P_{v,max}$ for *H. pluvialis* culture grown in optimal conditions in both AL-PBR and EOSS2 PBR, operated in chemostat mode, as a function of incident PFD. Experimental data are shown as mean ± SD, n = 3.

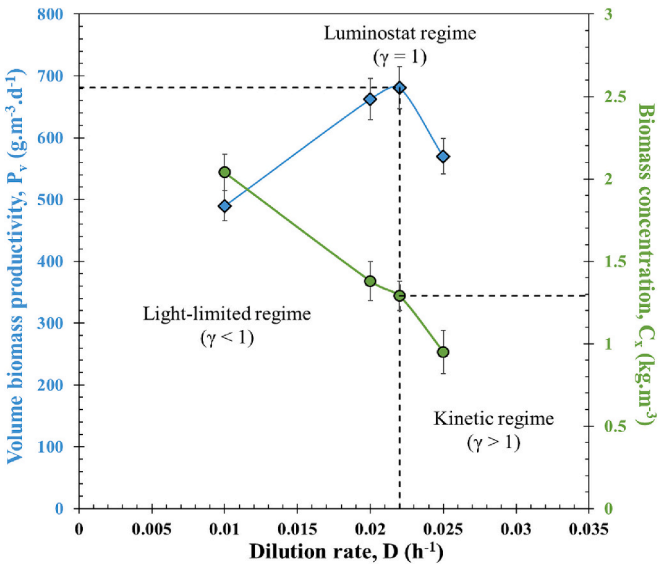

Fig. 9. Experimental determination of maximum biomass productivity $P_{v,max}$ and corresponding optimal biomass concentrations $C_{x,opt}$ by varying dilution rate D in the AL-PBR, operating in chemostat mode and illuminated with a PFD q = 200 µmol$_{hv}$.m^{-2}.s^{-1}. Data shown as mean ± SD, n = 3.

condition, the compensation point of photosynthesis A_c was then calculated using Eq. 12. As expected, the value of A_c was found to be near constant for all conditions, as a biological property of the cultivated strain (considering the uncertainty intrinsic to the overall determination method). For *H. pluvialis* (green phase), a value A_c of 650 ± 50 µmol$_{hv}$.kg^{-1}.s^{-1} was obtained.

Once the compensation point of photosynthesis A_c is known, the optimal biomass concentration $C_{x,opt}$ for each PFD value can be determined from Eq. 13. Fig. 10-a presents the $C_{x,opt}$ evolution of *H. pluvialis* obtained for different PFD values. Several experimental points were added. Close agreement with the predictions was observed for different growing conditions (error < 10 %). Using the approach, therefore, the optimal biomass concentration of *H. pluvialis* (green phase) can be determined from only one value of $C_{x,opt}$ obtained from a given PFD, for any other incident PFD value.

Eq. 14 can be used to determine the areal biomass concentrations $C^s_{x,opt}$ from $C_{x,opt}$ values where the specific illuminated surface of the culture system is known. The experimental $C^s_{x,opt}$ results for *H. pluvialis* grown in Al-PBR and EOSS-PBR are shown in Fig. 10-b with the predictions obtained from Eq. 14. Again, close agreement was observed between the experimental and predicted values. This also confirms the relevance of the areal biomass concentration. For a given PFD value, the same optimal areal biomass concentration $C^s_{x,opt}$ was obtained for the two different PBRs. Consequently, if the value is determined for a given PBR, it is easy to deduce the biomass concentration $C_{x,opt}$ for other PBRs with different specific illuminated surfaces (Eq. 14). This could also save a significant amount of time in determining the optimal operating conditions.

Finally, the determination of $C_{x,opt}$ can be combined with the prediction of maximum productivity to estimate the optimal dilution rate value as:

$$D_{opt} = \frac{P_{v,max}}{C_{x,opt}} \tag{15}$$

Fig. 10-c compares this prediction with the experimental values. Close agreement was again observed (error < 10 %).

3.3. Illustration of the significance with solar light - Picochlorum maculatum

3.3.1. Methodology

For the second case study, the microalgae strain *Picochlorum*

Table 2
Experimental values of maximum surface biomass productivities $P_{s,max}$, corresponding optimal biomass concentrations $C_{x,opt}$ and dilution rates D_{opt}, averaged mass absorption cross-sections E_a and compensation point of photosynthesis A_c obtained in both AL-PBR and EOSS2 PBR cultivating *H. pluvialis* at different incidents.

PBR	PFD, q ($\mu mol_{h\nu}.m^{-2}.s^{-1}$)	D_{opt} (h^{-1})	$C_{x,opt}$ ($kg.m^{-3}$)	$P_{s\ max}$ ($g.m^{-2}.d^{-1}$)	E_a ($m^2.kg^{-1}$)	A_c ($\mu mol_{h\nu}.kg^{-1}.s^{-1}$)
Al-PBR	75	0.02	0.62 ± 0.03	8.93 ± 0.54	155 ± 25	650
	100	0.02	0.79 ± 0.04	11.38 ± 0.58	125 ± 15	645
	130	0.021	0.95 ± 0.05	14.77 ± 1.74	100 ± 10	750
	200	0.022	1.29 ± 0.07	20.15 ± 2.06	80 ± 10	720
	300	0.025	1.68 ± 0.09	26.61 ± 2.84	65 ± 5	780
EOSS2	75	0.02	0.95 ± 0.04	9.12 ± 0.61	160 ± 20	570
	100	0.02	1.19 ± 0.05	11.42 ± 0.73	120 ± 10	690
	200	0.022	1.94 ± 0.08	20.21 ± 1.97	85 ± 10	650

maculatum, isolated from Qatar, was used, owing to its natural ability to thrive in a desert climate with high temperatures and PFDs. Previous studies have also demonstrated the ability of this strain to produce elevated amounts of proteins and essential polyunsaturated fatty acids even under extreme environmental conditions, making it a valuable local resource for fish feed [30]. The strain was therefore used to illustrate the value of our approach, using laboratory experiments to estimate the maximal biomass productivity achievable in large-scale outdoor biomass production.

The same approach as for *H.pluvialis* was used. Evolutions of areal productivity for *Picochlorum maculatum* were experimentally determined, based on the varying dilution rates for different PFD values and in continuous light (150, 300 and 600 $\mu mol_{h\nu}.m^{-2}.s^{-1}$). The experiments were carried out in continuous mode in a conical benchtop photobioreactor (ePBR, 101 Phenometrics, USA – Fig. 6-c) using enriched F/2 media as described by Rasheed et al. [30]. Samples were collected at fixed intervals throughout the experiment and biomass productivity was determined once steady state was achieved for a given dilution rate, by measuring the biomass concentration.

To validate the ability of our approach to estimate maximal biomass productivity in solar conditions (Eq. 11), additional experiments were carried out using the same PBR but with simulated day-night cycles. The detailed methodology can be found in Rasheed et al. [30]. In brief, diurnal variations in culture temperature along with PFD were applied to simulate conditions encountered in raceways for winter and summer periods in Qatar. The PFD cycles were obtained from a meteorological database, and the temperature cycles from a thermal modeling of outdoor raceways [40]. As described in Rasheed et al. [30], non-optimal temperature regimes can be encountered even in summer (too high temperature) or winter (too low temperature). Values for optimal and non-optimal temperature regimes were considered in this study (see the section below). Note that all samples for estimating biomass productivity were collected at the end of the light cycle, after the cultures had been exposed to maximum light.

3.3.2. Validation of method for estimating performance of culture systems in solar conditions

The maximal productivity values obtained in continuous light at different PFDs were used to determine the K' constant from Eq. 7. The results are given in Fig. 11. A K' value of 400 ± 20 $\mu mol_{h\nu}.m^{-2}.s^{-1}$ was obtained, demonstrating higher resistance of *Picochlorum maculatum* to high light intensity ($K' = 240$ $\mu mol_{h\nu}.m^{-2}.s^{-1}$ for *H.pluvialis*). Note that the ratio between minimum and maximum PFD values was set at 4, in accordance with the sensibility analysis given above (Fig. 4-b).

The values obtained in simulated day-night cycles were also added to Fig. 11. Because the configuration applied (fixed light source with time-varying PFD values) was simplified, calculation was fairly straightforward using Eq. 11. Normal incidence ($\cos(\theta) = 1$) was applied over the time with negligible diffuse light ($x_d = 0$). Only the PFD averaged on the day period was required, leading to $\overline{q} = 1485$ $\mu mol_{h\nu}.m^{-2}.s^{-1}$ and $\overline{q} = 1107$ $\mu mol_{h\nu}.m^{-2}.s^{-1}$ for the typical summer and winter PFD cycles respectively.

The theoretical determination of maximal productivity using the K' constant identified from constant light experiments was consistent with the values achieved in day-night cycles, but only for optimal temperature regimes. For non-optimal temperature regimes, the experimental productivities were found to be lower than the predicted ones. This demonstrates another advantage of our approach: by predicting the maximal productivity that can be achieved in given light conditions, the decrease in performance in non-ideal conditions (temperature regimes in this case) can be estimated. With *Picochlorum maculatum*, for example, a loss of productivity of around 40–50 % would be achieved in winter due to the culture temperature being too low. As discussed by Raheed et al. [30,41], this could be attenuated by adding thermal regulation units. Our approach could be useful in this case: by predicting productivity with and without thermal regulation, useful information would be obtained to conduct a techno-economic analysis of the advantages of such an investment [41].

3.3.3. Estimating outdoor performance from a meteorological database

In the section above, Eq. 11 was simplified because of the simulated day-night cycle provided by a fixed LED panel on the lab-scale PBR. Eq. 11 can also replicate the effects of other outdoor culture phenomena in sunlight, such as changes in PFD, direct/diffuse light distribution (due to clouds, for example) and incident angle over the year. To illustrate this, an outdoor culture system (Fig. 6-d) located in Al-Khor in Qatar (N 25°69, E 51°51) was used. The aim was to estimate the evolution of maximal productivity exploitation over a year achievable with *Picochlorum maculatum*. To obtain average monthly values, for example (any other period could be used), input data in terms of PFD $\overline{q}$ (here in the PAR), $\overline{\cos(\theta)}$ and $\overline{x_d}$ were determined by averaging a time series of corresponding data over a given month (as above, the average was taken only during daytime periods). These values were used to determine maximal productivity using Eq. 11 (using $P_{s\ max\ 1} = 7.16$ $g.m^{-2}.d^{-1}$ arbitrarily as the reference, as obtained in constant light for a PFD of $q = 150 \mu mol_{h\nu}.m^{-2}.s^{-1}$). In addition, as an example of other useful data with the techno-economic analysis, the photosynthetic conversion efficiency *PE* was added, using [41,42]:

$$PE = \frac{P_S \Delta H_C^0}{SI_{PAR}} \tag{16}$$

where ΔH_C^0 is the enthalpy of biomass combustion (22.5 $J.g^{-1}$) and SI_{PAR} the daily solar irradiation ($kJ.m^{-2}.day^{-1}$), calculated for a horizontal surface and within the PAR range (400 to 700 nm, 43 % of the total sunlight spectrum).

Fig. 12 and Table 3 give the biomass productivity evolution and resulting photosynthetic conversion efficiency over the months, with greater productivities in summer (an increase of around 60 %) but a lower photosynthetic conversion efficiency (a decrease of around 25 %) as the combined effect of the evolutions in both biomass productivity and solar irradiation. From these results, the achievable biomass production over a year of exploitation (4.64 $kg.m^{-2}.year^{-1}$, around 46 t. $ha^{-1}.year^{-1}$), and the average value of photosynthetic conversion

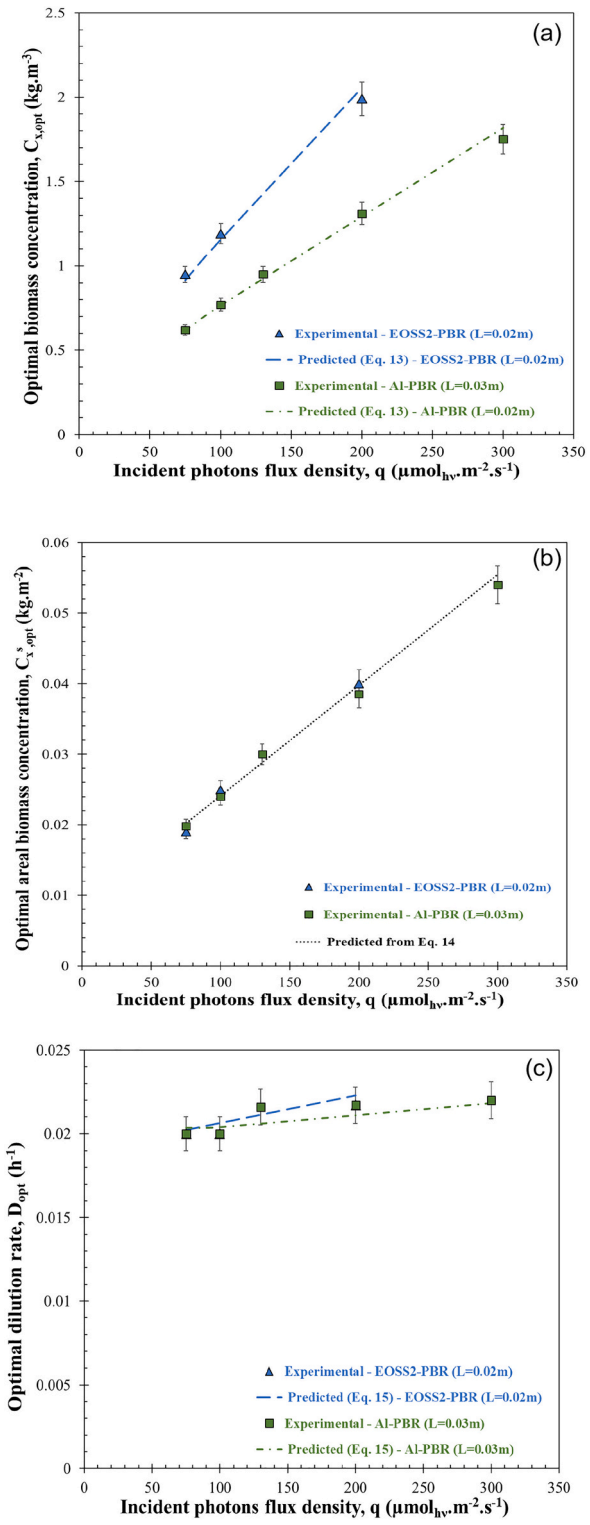

Fig. 10. Experimental and predicted values of optimal biomass concentration $C_{x,opt}$ (10-a), optimal areal biomass concentration $C^s_{x,opt}$ (10-b) and optimal dilution rate D_{opt} (10-c) for *H. pluvialis* culture grown in optimal conditions in both AL-PBR and EOSS2 PBR, operated in chemostat mode, as a function of incident PFD. Experimental data shown as mean ± SD, n = 3.

efficiency (around 1.3 %) can be estimated.

To illustrate the advantage of using Eq. 11 for meaningful representation of sunlight conditions, the values predicted without the influence of diffuse light ($x_d = 0$) and incident angle ($cos\theta = 1$) were added. As discussed previously by Pruvost et al. [19], this leads to a

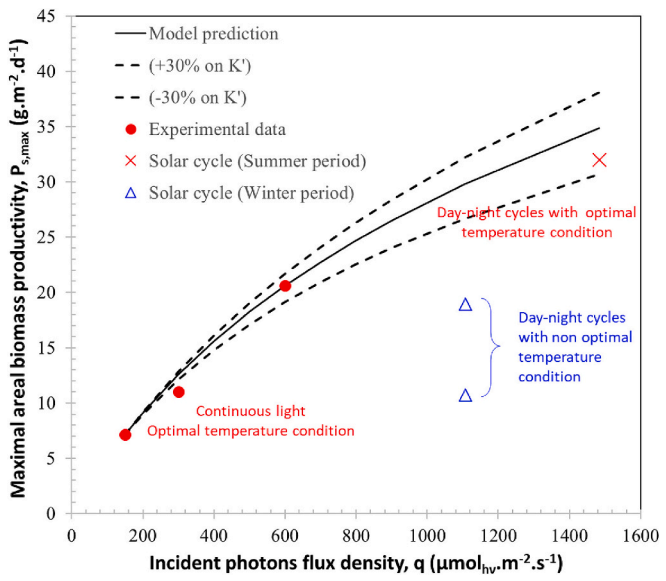

Fig. 11. Experimental and predicted values of maximal areal biomass productivity $P_{s,max}$ for *Picochlorum maculatum* culture grown in optimal conditions in conical benchtop PBR, operated in chemostat mode, as a function of incident photons flux density q. Values obtained for both constant light and simulated day-night cycles.

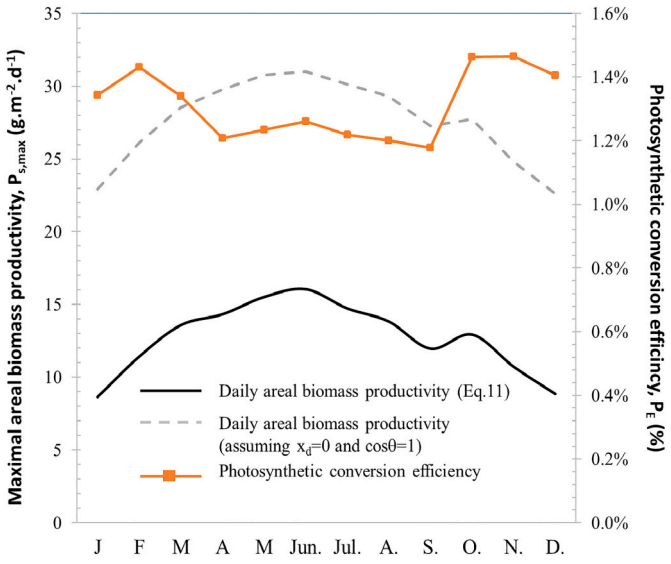

Fig. 12. Prediction of yearly evolution of maximal biomass productivities and photosynthetic conversion efficiency for the strain *Picochlorum maculatum* cultivated in solar conditions at Al-Khor location in Qatar. Values given for a horizontal culture system. Biomass productivities, disregarding the influence of diffuse light ($x_d = 0$) and incident angle ($cos\theta = 1$), provided for information (see text for details).

significant over-estimation of biomass productivity (a factor of around 2 in this case).

4. Conclusions

A simplified new method for determining the maximal performance (volumetric and areal biomass productivity) and corresponding optimal operating points (biomass concentration, dilution rate) for a given culture system (characterized by specific illuminated surface a_{light} and design dark fraction f_d), strain and culture conditions (including solar)

Table 3
Monthly averaged values of solar irradiation conditions for horizontal culture systems operated in Al-Khor (Qatar) and corresponding predicted values of maximal biomass productivities and photosynthetic conversion efficiency for *Picochlorum maculatum*.

Month	PFD	cos(θ)	x_d	P_S	Solar irradiation	PE (%)
	($\mu mole_{h\nu}.m^{-2}.s\text{-}1$)	(no unit)	(no unit)	($g.m^{-2}.d^{-1}$)	($kJ.m^{-2}.d^{-1}$)	(no unit)
January	709	0.47	0.48	8.6	14,454	1.34 %
February	880	0.55	0.43	11.4	17,935	1.43 %
March	1026	0.61	0.40	13.6	22,802	1.34 %
April	1107	0.64	0.41	14.3	26,651	1.21 %
May	1174	0.64	0.37	15.5	28,260	1.23 %
June	1190	0.65	0.36	16.0	28,649	1.26 %
July	1129	0.65	0.40	14.7	27,180	1.22 %
August	1075	0.66	0.43	13.8	25,884	1.20 %
September	948	0.65	0.47	12.0	22,835	1.18 %
October	975	0.56	0.39	12.9	19,872	1.46 %
November	808	0.50	0.41	10.7	16,459	1.46 %
December	695	0.44	0.45	8.8	14,152	1.41 %

has been presented and validated. The approach combines engineering equations smartly adapted to eliminate parameters that are difficult to obtain, with a few conventional small-scale experiments, to determine the remaining key parameters relative to the strain.

Since the information required by experimental campaigns usually takes several weeks to obtain, this method represents significant savings in terms of time, while producing predictions within an acceptable range of accuracy for most engineering purposes (a deviation of below 10 % was found in all cases). The proposed method, which is fairly simple to apply, appears to be a relevant tool for understanding and analyzing PBR behaviors together with accelerating the scaling-up of any microalgae culture.

It should be borne in mind, of course, that the approach is only valid for estimating maximal biomass productivity. In other words, this means that it only concern the productivities obtained without nutrient limitation, and for temperature and pH ranges close to the optimal. In a sense, it can be considered optimistic, considering all the issues that could potentially be encountered in outdoor conditions (especially in the desert), but the information may still be useful for estimating the maximal potential of a given strain or loss of performance caused by non-optimal culture conditions (as illustrated here with *Picochlorum maculatum* where a loss of productivity of around 40–50 % was observed due to sub-optimal temperature). For more detailed representations (such as effect of temperature, daytime period, pigment acclimation, etc.), other modeling approaches should be used (as proposed by other authors, see [12], but they would not offer the same simplicity of use, which is the primary objective of the present approach.

CRediT authorship contribution statement

J. Pruvost: Writing – review & editing, Writing – original draft, Visualization, Validation, Software, Methodology, Investigation, Funding acquisition, Formal analysis, Data curation, Conceptualization. **R. Rasheed:** Investigation. **K. Samhat:** Investigation. **A. Kazbar:** Writing – review & editing. **H. Al Jabri:** Writing – review & editing. **J. Dauchet:** Writing – review & editing. **J.F. Cornet:** Writing – review & editing.

Declaration of competing interest

The authors declare that they have no known competing financial interests or personal relationships that could have appeared to influence the work reported in this paper.

Data availability

Data will be made available on request.

Acknowledgments

This work was supported by the DISCUS project of the NExT Initiative (Nantes Excellence Trajectory) International Research Partnership and by the International Research Center "Innovation Transportation and Production Systems" of the I-SITE CAP 20-25 (ANR-16-IDEX-0001).

Appendix A. Demonstration of general equations using any degree of collimation n for the local rate of photon absorption (RPA) A(z) and mean volumetric photon absorption rate (MVRPA) $<\mathscr{A}>$ in 1D Cartesian geometry

This appendix is proposed to establish the equations to use for local profiling of the rate of photon absorption (RPA), and consequently the mean volumetric rate of photon absorption in a 1D Cartesian PBR, in general (i.e. flat panel culture system), with any angular distribution for the incident PFD. To the best of our knowledge, this approach has never been proposed before.

An angular dependence for the incident luminance (or intensity) $I_0(\theta)$ must first be assumed on the surface of the culture system (at the boundary z = 0) from a cosine modulation of n^{th} order [16,29] in the form:

$$I(\theta)_{|z=0} = I_0 cos^n(\theta) \tag{A1}$$

The dependence of the azimuth angle ϕ is not considered here because, in most practical cases, both the radiative properties and radiative transfer are independent in terms of azimuth (especially when edge effects are negligible). This approach enables consideration of any general situation for the source of the radiative transfer problem between two extreme situations: i) the well-known quasi collimated incidence with $n = \infty$, then $I(\theta)_{|z=0} = I_0\delta(\theta - \theta_C)$ where the incident radiation exists only in the θ_C direction, and ii) the diffuse Lambertian incidence with $n = 0$ and $I(\theta)_{|z=0} = I_0$ for any angle θ. All the demonstrations in this appendix assume a grey absorbing medium characterized by a mean mass absorption coefficient Ea averaged on the PAR (see appendix B for the determination considered).

A.1. Some definitions and equations between intensity (luminance), irradiance, photon flux density and photon absorption rates in 1D Cartesian radiative transfer

All the radiative physical observables are defined from the intensity I(θ), which is an angular quantity depending only on the angular distribution of the light source (boundary) with an absorbing medium (Pruvost and Cornet, 2012). For a 1D Cartesian geometry with incidence on one side of z = 0, the irradiance is first given by the integral:

$$G = \int_0^{2\pi} \int_0^{\pi/2} I(\theta) sin(\theta) d\theta \, d\phi = 2\pi \int_0^{\pi/2} I(\theta) sin(\theta) d\theta \tag{A2}$$

Second, the hemispherical photon flux density (a vector projection in the z direction) is also independent in terms of azimuth and given by the first moment of the angular intensity:

$$q = 2\pi \int_0^{\pi/2} I(\theta) cos(\theta)\ sin(\theta) d\theta \tag{A3}$$

These definitions can be used at the boundary (input wall of the PBR with z = 0) to relate the incident intensity I_0 in a general angular situation to the incident PFD q_0. Using Eq. A1 in Eq. A3 leads to the following:

$$q_0 = 2\pi \int_0^{\pi/2} I_0(\theta) cos(\theta)\ sin(\theta) d\theta = 2\pi I_0 \int_0^{\pi/2} cos^{n+1}(\theta)\ sin(\theta) d\theta = \frac{2\pi I_0}{n+2}$$

Thus

$$I_0 = \frac{n+2}{2\pi}\, q_0 \tag{A4}$$

Note here that when n goes to infinity, the intensity becomes a delta Dirac function with respect to incidence angle θ and the value of I_0 cannot be directly interpreted, when outside an integral. As a consequence, q_0 does not tend towards 0 when n approaches infinity, since I_0 also approaches infinity.

Finally, in general terms, the irradiance $G(z)$ defined by Eq. (A2) can be used to form many significant physical quantities related to photon absorption rates, which are the basis of the kinetic and energetic formulation combinations in the PBR (Pruvost and Cornet, 2012; Dauchet et al., 2016). The specific local rate of photon absorbed A [$\mu mol_{h\nu}.kg^{-1}.s^{-1}$] (referred to as the RPA in the body of the article) is simply obtained from the mass absorption coefficient Ea (see also appendix B and Eq. 12):

$$A(z) = Ea\, G(z) \tag{A5}$$

This quantity is easily related to the local volumetric photon absorption rate $\mathscr{A}$ [$\mu mol_{h\nu}.m^{-3}.s^{-1}$] by multiplying it by the biomass dry weight concentration C_X:

$$\mathscr{A}(z) = Ea\, C_X G(z) = k_a\, G(z) \tag{A6}$$

where the linear absorption coefficient $k_a = Ea\, C_X$ [m^{-1}] has been introduced.

To establish energy balances in the culture system, an average of this local volumetric rate provides the mean volumetric rate of photons absorbed $<\mathscr{A}>$ (called MVRPA):

$$<\mathscr{A}> = \frac{1}{L}\int_0^L \mathscr{A}(z) dz = \frac{1}{L} Ea\, C_X \int_0^L G(z) dz \tag{A7}$$

From an energy balance on the photon phase, it has been also demonstrated [16] that the MVRPA can alternatively be expressed as:

$$<\mathscr{A}> = (1 - f_d) q_0\, a_{light} p_A = (1 - f_d) <\mathscr{A}>_{max} p_A \tag{A8}$$

where the design dark volume fraction of the culture system f_d, and absorptivity p_A corresponding to the proportion of incident photons absorbed in the culture volume have been introduced.

A.2. Bouguer law and establishment of equations for irradiance G(z) and RPA A(z) profiles in a 1D Cartesian geometry

The well-known Bouguer law (often incorrectly referred as the Lambert-Beer law) gives the attenuation of the intensity (and not for the irradiance or the flux density) in an absorbing medium for any direction forming an angle θ with the norm by (using Eq. A1):

$$I(z) = I_0 cos^n(\theta) exp\left(-\frac{k_a z}{cos(\theta)}\right) = I_0 cos^n(\theta) exp\left(-\frac{Ea\, C_X z}{cos(\theta)}\right) \tag{A9}$$

From this profile of intensity in the direction θ, it is then easy to establish the equation for the irradiance $G(z)$ by taking an average of all the θ directions, using Eq. A2:

$$G(z) = 2\pi \int_0^{\pi/2} I(\theta, z) sin(\theta) d\theta = 2\pi \int_0^{\pi/2} I_0 cos^n(\theta) exp\left(-\frac{k_a z}{cos(\theta)}\right) sin(\theta) d\theta \tag{A10}$$

Using Eq. A4 to eliminate I_0 and applying the variable change $\mu = \cos(\theta)$ leads to the following analytic solution for the irradiance profile:

$$G(z) = (n+2) q_0 \int_0^1 \mu^n exp\left(-\frac{k_a z}{\mu}\right) d\mu = (n+2) q_0\, E_{n+2}(k_a z) \tag{A11}$$

where the E_N function is the n^{th} order integral exponential function available in many languages, and software (Matlab®, Mathematica, Maple, etc.).

Finally, this leads to the general expression for the local RPA (for any degree of collimation n at the source):

$$A(z) = Ea\ (n+2) q_0\ E_{n+2}(k_a z) \tag{A12}$$

A.3. Establishment of general equation for mean volumetric rate of photon absorption (MVRPA) $<\mathscr{A}>$ in a 1D Cartesian geometry

Once the local expression for the RPA A(z) is established (Eq. A12), this rate can be spatially averaged to obtain the MVRPA as the main physical quantity available for energy balances in the culture system (using Eqs. A5 and A7):

$$<\mathscr{A}>=\frac{1}{L}\int_0^L \mathscr{A}\,(z)dz = \frac{1}{L}\,C_X \int_0^L A(z)dz \tag{A13}$$

Substituting Eq. A12 into Eq. A13 gives:

$$<\mathscr{A}>=\frac{(n+2)\,q_0}{L}\int_0^L k_a\,E_{n+2}(k_a z)dz$$

$$=\frac{(n+2)\,q_0}{L}\left[\frac{1}{n+2}-E_{n+3}(k_a\,L)\right]$$

i.e.:

$$<\mathscr{A}>=q_0\,a_{light}\,[1-(n+2)\,E_{n+3}(k_a\,L)\,] \tag{A14}$$

This final form of the MVRPA can be compared to Eq. A8 and by identification (assuming no dark fraction in the culture system), a theoretical expression of the absorptivity is obtained:

$$p_A = [1-(n+2)\,E_{n+3}(k_a\,L)\,] \tag{A15}$$

A.4. Behavior of general established equations with variable degree of collimation n for the two extreme cases: the quasi collimated ($n = \infty$) and diffuse Lambertian ($n = 0$) light incidences

All the general equations established in this appendix for irradiance $G(z)$, local RPA $A(z)$ and MVRPA $<\mathscr{A}>$ (regarding degree of collimation n) necessarily lead to recognized equations for the two simple extreme values of n.

First, with the quasi-collimated incidence for q_0, $n\to\infty$ and using the properties for the n^{th} order integral exponential function $\lim_{n\to\infty}[n\,E_n(x)\,] = e^{-x}$ and $\lim_{n\to\infty}[E_n(x)\,] = 0$:

$$G(z) = q_0\,e^{-k_a z}, k_a = Ea\,C_X$$

$$A(z) = Ea\,q_0\,e^{-k_a z}$$

and

$$<A>=q_0 a_{light}\left[1-e^{-k_a L}\right] \tag{A15}$$

in accordance with Eq. 11 in the body of the article, and with the Bouguer law as explained above.

Second, the opposite situation where $n = 0$ corresponds to the diffuse Lambertian incidence for q_0. In this case, the recursive properties can be used:

$$2E_3(x) = e^{-x} - x\,E_2(x)$$
$$E_2(x) = e^{-x} - x\,E_1(x)$$
$$x\,E_1(x) = -x\,E_i(-x)$$

where $E_i(x)$ is the exponential integral function, to rewrite Eq. A12 and A14 with $n = 0$ in the form:

$$A(z) = 2\,Ea\,q_0\,\left[e^{-k_a z} + k_a z\,E_i(-k_a z)\right]$$

$$<\mathscr{A}>=q_0 a_{light}\left[1-e^{-k_a L}(1-k_a L)+(k_a L)^2\,E_i(-k_a L)\right] \tag{A16}$$

These two equations for diffuse incidence and grey absorbing medium are well known and have been obtained by other methods with chemical photoreactors [43].

Appendix B. Explanation for the experimental and theoretical protocol in assessing the mean grey averaged mass absorption coefficient Ea from spectroscopic measurements

The purpose of this appendix is to assemble all the theoretical and experimental information in order to access the spectral mass absorption

coefficients Ea_λ and their equivalent grey averaged value Ea, by inverting the measurement of transmittances in the single scattering condition. All these points have already been extensively discussed in the literature, in particular by the Laurent Pilon team (see for example [25,44] and are simply recalled here for convenience, to support the body of the article.

B.1. Theoretical approach for inversion of normal-hemispherical transmittance measurements within the limit of single scattering assumption

The single scattering assumption is theoretically verified if any illuminated microalgae suspension with an incident collimated beam of wavelength λ is sufficiently optically thin to observe either no interaction with a scatterer (ballistic photons leading to a transmittance $T_{\lambda,0}$) or only one interaction (a scattering event leading to a transmittance $T_{\lambda,1}$ and a reflectance $R_{\lambda,1}$).

The following classical radiative properties are first introduced:

- $ka_\lambda = Ea_\lambda C_X$, the linear absorption coefficient
- $ks_\lambda = Es_\lambda C_X$, the linear scattering coefficient
- $kext_\lambda = ka_\lambda + ks_\lambda$, the linear extinction coefficient
- b, the backscattered fraction for scattering obtained from the phase function of the particle [26]
- f, the forward scattered fraction $f = 1\text{-}\ b$

This allows the transmittance and reflectance expressions for photons experiencing one or no scattering event (with a medium of thickness L) to be expressed as:

- for ballistic photons, $T_{\lambda,0} = exp(-kext_\lambda L) \cong 1 - kext_\lambda L$ at the optical thin limit
- for scattered transmitted photons, $T_{\lambda,1} = ks_\lambda Lf$ and for reflected one $R_{\lambda,1} = ks_\lambda Lb$

In practical terms, a spectrophotometer equipped with an integrating sphere measures both normal-hemispherical transmittance $T_{\lambda,NH}$ and normal-hemispherical reflectance $R_{\lambda,NH}$.

At the single scattering limit, the photons experiencing more than one scattering event can be disregarded, and one has:

$$T_{\lambda,NH} = T_{\lambda,0} + T_{\lambda,1} \tag{B1}$$

$$R_{\lambda,NH} = R_{\lambda,1} \tag{B2}$$

For the 1D Cartesian approximation generally assumed in spectrophotometry, the exiting photons transmitted or reflected are therefore given by the following equation:

$$T_{\lambda,NH} + R_{\lambda,NH} = T_{\lambda,0} + T_{\lambda,1} + R_{\lambda,1} \tag{B3}$$

which may be written from the radiative properties:

$$T_{\lambda,NH} + R_{\lambda,NH} = 1 - kext_\lambda L + ks_\lambda L\,(f + b) \tag{B4}$$

Because by definition $(f + b) = 1$, we have:

$$T_{\lambda,NH} + R_{\lambda,NH} = 1 - ka_\lambda L - ks_\lambda L + ks_\lambda L = 1 - ka_\lambda L \tag{B5}$$

Finally, because $ka_\lambda = Ea_\lambda C_X$, the spectral mass absorption coefficient Ea_λ can be obtained by omitting the reflectivity for the single scattering condition only from the knowledge of the normal-hemispherical transmittance $T_{\lambda,NH}$:

$$Ea_\lambda = \frac{1 - T_{\lambda,NH} - R_{\lambda,NH}}{C_X L} \cong \frac{1 - T_{\lambda,NH}}{C_X L} \cong \frac{ln(10) OD_\lambda}{C_X L} \tag{B6}$$

where OD_λ is the absorbance or optical density given by the spectrophotometer.

Unlike inversion of the extinction or scattering coefficients, which is debated in the literature, Eq. B6 is widely accepted as inverting a transmittance measurement to obtain the mass absorption coefficient [25,44].

B.2. Experimental procedure at spectrophotometer

To carry out experiments according to the single scattering approximation, it is essential to start by measuring $T_{\lambda,NH}$ by successive dilution of a sample [44]. By reducing the biomass concentration C_X in the sample, the single scattering approximation conditions are gradually approached. In doing so, however, the value of the transmittance tends towards 1, which is nearing the experimental limits of the spectrophotometer. The right concentration must therefore be found, representing the best compromise between dilution and accuracy and allowing inversion of the mass absorption coefficient by the approximate theoretical formula Eq. B6. In other words, when we superimpose the inverted curves of the mass absorption coefficient as a function of the wavelength, we will obtain spectra which overlap from a certain concentration limit [44]. If the uncertainties on the spectrum become too high, the results obtained with too-low biomass concentrations are not considered (in practice, a biomass concentration ranging from 0.02 to 0.07 $kg.m^{-3}$ is retained for microalgae).

B.3. Mean mass absorption grey coefficient Ea

The method described above leads to a spectrum of mass absorption coefficient, i.e. spectral values of this coefficient Ea_λ in the PAR. If work with a grey approximation for the incident light absorption is required, a mean grey mass absorption coefficient Ea must be defined in the PAR. All that's

required for this is the incident spectral photon distribution of source p_λ (given by the norm AM 1.5 for solar incidence or by the supplier of any artificial source). The mean mass absorption coefficient is then simply obtained by:

$$E_a = \frac{\int_{400\ nm}^{700\ nm} Ea_\lambda p_\lambda d\lambda}{\int_{400\ nm}^{700\ nm} p_\lambda d\lambda} \tag{B7}$$

where the term $\int_{400\ nm}^{700\ nm} p_\lambda d\lambda = 1$ if p_λ is normalized as a probability density function (pdf).

References

[1] M.C. Pina-Pérez, W.M. Brück, T. Brück, M. Beyrer, Chapter 4- microalgae as healthy ingredients for functional foods, in: C.M. Galanakis (Ed.), The Role of Alternative and Innovative Food Ingredients and Products in Consumer Wellness, Academic Press, 2019, pp. 103–137.

[2] D. Jha, V. Jain, B. Sharma, A. Kant, V.K. Garlapati, Microalgae-based pharmaceuticals and nutraceuticals: an emerging field with immense market potential, ChemBioEng Reviews 4 (2017) 257–272.

[3] D.A. Wood, Microalgae to biodiesel - review of recent progress, Bioresource Technology Reports 14 (2021) 100665.

[4] R.H. Wijffels, M.J. Barbosa, An outlook on microalgal biofuels, Science 329 (2010) 796–799.

[5] S.F. Mohsenpour, S. Hennige, N. Willoughby, A. Adeloye, T. Gutierrez, Integrating micro-algae into wastewater treatment: a review, Sci. Total Environ. 752 (2021) 142168.

[6] P. Darvehei, P.A. Bahri, N.R. Moheimani, Model development for the growth of microalgae: a review, Renew. Sust. Energ. Rev. 97 (2018) 233–258.

[7] A. Malek, L.C. Zullo, P. Daoutidis, Modeling and dynamic optimization of microalgae cultivation in outdoor open ponds, Ind. Eng. Chem. Res. 55 (2015) 3327–3337.

[8] G. Luzi, C. McHardy, Modeling and simulation of Photobioreactors with computational fluid dynamics—a comprehensive review, Energies 15 (2022) 3966.

[9] J. Legrand, A. Artu, J. Pruvost, A Review on Photobioreactor Design and Modelling for Microalgae Production, Reaction Chemistry & Engineering, 2021.

[10] J. Pruvost, J.F. Cornet, Knowledge models for engineering and optimization of photobioreactors, in: C.P.A.C. Walter (Ed.), Microalgal Biotechnology, De Gruyter GmbH & Co. KG, 2012, pp. 181–224.

[11] J. Dauchet, J.-F. Cornet, F. Gros, M. Roudet, C.-G. Dussap, Chapter one-Photobioreactor modeling and radiative transfer analysis for engineering purposes, in: J. Legrand (Ed.), Advances in Chemical Engineering, Academic Press, 2016, pp. 1–106.

[12] J. Pruvost, J.F. Cornet, F. Le Borgne, V. Goetz, J. Legrand, Theoretical investigation of microalgae culture in the light changing conditions of solar photobioreactor production and comparison with cyanobacteria, Algal Res. 10 (2015) 87–99.

[13] A. Soulies, C. Castelain, T.I. Burghelea, J. Legrand, H. Marec, J. Pruvost, Investigation and modeling of the effects of light spectrum and incident angle on the growth of *Chlorella vulgaris* in photobioreactors, Biotechnol. Prog. 32 (2016) 247–261.

[14] H. Takache, J. Pruvost, J.F. Cornet, Kinetic modeling of the photosynthetic growth of Chlamydomonas reinhardtii in a photobioreactor, Biotechnol. Prog. 28 (2012) 681–692.

[15] A. Busnel, K. Samhat, E. Gérard, A. Kazbar, H. Marec, E. Dechandol, B. Le Gouic, J. L. Hauser, J. Pruvost, Development and validation of a screening system for characterizing and modeling biomass production from cyanobacteria and microalgae: application to Arthrospira platensis and Haematococcus pluvialis, Algal Res. 58 (2021) 102386.

[16] J.F. Cornet, C.G. Dussap, A simple and reliable formula for assessment of maximum volumetric productivities in photobioreactors, Biotechnol. Prog. 25 (2009) 424–435.

[17] J. Pruvost, J.F. Cornet, V. Goetz, J. Legrand, Theoretical investigation of biomass productivities achievable in solar rectangular photobioreactors for the cyanobacterium *Arthrospira platensis*, Biotechnol. Prog. 28 (2012) 699–714.

[18] J. Pruvost, G. Van Vooren, B. Le Gouic, A. Couzinet-Mossion, J. Legrand, Systematic investigation of biomass and lipid productivity by microalgae in photobioreactors for biodiesel application, Bioresour. Technol. 102 (2011) 150–158.

[19] J. Pruvost, J.F. Cornet, V. Goetz, J. Legrand, Modeling dynamic functioning of rectangular photobioreactors in solar conditions, AICHE J. 57 (2011) 1947–1960.

[20] J. Pruvost, F. Le Borgne, A. Artu, J. Legrand, Development and characterization of a thin-film solar photobioreactor (AlgoFilm©) based on process intensification principles, Algal Res. (2017) 120–137.

[21] H. Takache, G. Christophe, J.F. Cornet, J. Pruvost, Experimental and theoretical assessment of maximum productivities for the microalgae Chlamydomonas reinhardtii in two different geometries of photobioreactors, Biotechnol. Prog. 26 (2010) 431–440.

[22] J. Dauchet, S. Blanco, J.-F. Cornet, R. Fournier, Calculation of the radiative properties of photosynthetic microorganisms, J. Quant. Spectrosc. Radiat. Transf. 161 (2015) 60–84.

[23] J. Dauchet, J.-F. Cornet, F. Gros, M. Roudet, C.-G. Dussap, Photobioreactor modeling and radiative transfer analysis for engineering puposes, Advanced Chem. Eng. J. 48 (2016) 1–106.

[24] H. Berberoglu, P.S. Gomez, L. Pilon, Radiation characteristics of Botryococcus braunii, Chlorococcum littorale, and Chlorella sp. used for fixation and biofuel production, J. Quant. Spectrosc. Radiat. Transf. 110 (2009) 1879–1893.

[25] R. Kandilian, J. Pruvost, A. Artu, C. Lemasson, J. Legrand, L. Pilon, Comparison of experimentally and theoretically determined radiation characteristics of photosynthetic microorganisms, J. Quant. Spectrosc. Radiat. Transf. 175 (2016) 30–45.

[26] L. Pottier, J. Pruvost, J. Deremetz, J.F. Cornet, J. Legrand, C.G. Dussap, A fully predictive model for one-dimensional light attenuation by Chlamydomonas reinhardtii in a torus photobioreactor, Biotechnol. Bioeng. 91 (2005) 569–582.

[27] J. Pruvost, F. Le Borgne, A. Artu, J.-F. Cornet, J. Legrand, Industrial photobioreactors and scale-up concepts, Advances in Chemical Engineering-photobioreaction Engineering, Elsevier 2016, pp. 257–310.

[28] H. Takache, G. Christophe, J.F. Cornet, J. Pruvost, Experimental and theoretical assess- ment of maximum productivities for the micro-algae Chlamydomonas reinhardtii in two different geometries of photobioreactors, Biotechnol. Prog. 26 (2010) 431–440.

[29] J.-F. Cornet, Calculation of optimal design and ideal productivities of volumetrically lightened photobioreactors using the constructal approach, Chem. Eng. Sci. 65 (2010) 985–998.

[30] R. Rasheed, M. Thaher, N. Younes, T. Bounnit, K. Schipper, G.K. Nasrallah, H. Al Jabri, I. Gifuni, O. Goncalves, J. Pruvost, Solar cultivation of microalgae in a desert environment for the development of techno-functional feed ingredients for aquaculture in Qatar, Sci. Total Environ. 835 (2022) 155538.

[31] J. Pruvost, Cultivation of algae in photobioreactors for biodiesel production, in: E. I. USA (Ed.), Biofuels: Alternative Feedstocks and Conversion Processes, A Pandey, C Larroche, SC Ricke and CG Dussap, 2011, pp. 439–464.

[32] J.F. Cornet, C.G. Dussap, J.B. Gros, Conversion of radiant light energy in photobioreactors, AICHE J. 40 (1994) 1055–1066.

[33] J.F. Cornet, C.G. Dussap, P. Cluzel, G. Dubertret, A structured model for simulation of cultures of the cyanobacterium Spirulina platensis in photobioreactors. 1. Coupling between light transfer and growth kinetics, Biotechnol. Bioeng. 40 (1992) 817–825.

[34] B. Degrenne, J. Pruvost, G. Christophe, J.-F. Cornet, G. Cogne, J. Legrand, Investigation of the combined effects of acetate and photobioreactor illuminated fraction in the induction of anoxia for hydrogen production by Chlamydomonas reinhardtii, Int. J. Hydrog. Energy 35 (2010) 10741–10749.

[35] R. Kandilian, A. Soulies, J. Pruvost, B. Rousseau, J. Legrand, L. Pilon, Simple method for measuring the spectral absorption cross-section of microalgae, Chem. Eng. Sci. 146 (2016) 357–368.

[36] E. Lee, J. Pruvost, X. He, R. Munipalli, L. Pilon, Design tool and guidelines for outdoor photobioreactors, Chem. Eng. Sci. 106 (2014) 18–29.

[37] J. Hoeniges, W. Welch, J. Pruvost, L. Pilon, A novel external reflecting raceway pond design for improved biomass productivity, Algal Res. 65 (2022) 102742.

[38] J. Pruvost, J.F. Cornet, L. Pilon, Large scale production of algal biomass: Photobioreactors, in: U. Springer (Ed.), Algae Biotechnology: Products and Processes, 2016, pp. 41–66.

[39] M. Bonnanfant, H. Marec, B. Jesus, J.-L. Mouget, J. Pruvost, Investigation of the photo- synthetic response of Chlorella vulgaris to light changes in a torus-shape photobioreactor, Appl. Microbiol. Biotechnol. 105 (2021) 8689–8701.

[40] J. Pruvost, V. Goetz, A. Artu, P. Das, H. Al Jabri, Thermal modeling and optimization of microalgal biomass production in the harsh desert conditions of State of Qatar, Algal Res. 38 (2019) 101381.

[41] R. Rasheed, K. Schippera, I. Gifuni, H. Al Jabri, M. Barbosa, O. Gonçalves, J. Pruvost, Thermal regulation of algae cultures in raceway ponds utilizing ground heat: improving techno-economic feasibility and process sustainability of large-scale algae production in Qatar, Sustain Energy Technol Assess 60 (2023) 103497.

[42] K. Schipper, H.M.S.J. Al-Jabri, R.H. Wijffels, M.J. Barbosa, Techno-economics of algae production in the Arabian peninsula, Bioresour. Technol. 331 (2021) 125043.
[43] V. Rochatte, G. Dahi, A. Eskandari, J. Dauchet, F. Gros, M. Roudet, J.F. Cornet, Radiative transfer approach using Monte Carlo method for actinometry in complex geometry and its application to Reinecke salt photodissociation within innovative pilot-scale photo (bio)reactors, Chem. Eng. J. 308 (2017) 940–953.
[44] H. Berberoglu, L. Pilon, Experimental measurements of the radiation characteristics of Anabaena variabilis ATCC 29413-U and Rhodobacter sphaeroides ATCC 49419, Int. J. Hydrog. Energy 32 (2007) 4772–4785.